

TI-1087

WADC TECHNICAL REPORT 54-20

AD0039439 \*

✓  
39439

RECEIVED  
TECHNICAL  
CONFERENCE

Wright-Patterson  
Technical Library  
WPAFB, OHIO 45433

~~CONFIDENTIAL~~  
ASAPRL

FATIGUE FAILURE UNDER RESONANT  
VIBRATION CONDITIONS

B. J. LAZAN

UNIVERSITY OF MINNESOTA

Statement A  
Approved for Public Release

MARCH 1954

20050713166

WRIGHT AIR DEVELOPMENT CENTER

ENCL. (2)

## NOTICES

When Government drawings, specifications, or other data are used for any purpose other than in connection with a definitely related Government procurement operation, the United States Government thereby incurs no responsibility nor any obligation whatsoever; and the fact that the Government may have formulated, furnished, or in any way supplied the said drawings, specifications, or other data, is not to be regarded by implication or otherwise as in any manner licensing the holder or any other person or corporation, or conveying any rights or permission to manufacture, use, or sell any patented invention that may in any way be related thereto.

The information furnished herewith is made available for study upon the understanding that the Government's proprietary interests in and relating thereto shall not be impaired. It is desired that the Judge Advocate (WCJ), Wright Air Development Center, Wright-Patterson Air Force Base, Ohio, be promptly notified of any apparent conflict between the Government's proprietary interests and those of others.

WADC TECHNICAL REPORT 54-20

FATIGUE FAILURE UNDER RESONANT  
VIBRATION CONDITIONS

B. J. LAZAN  
UNIVERSITY OF MINNESOTA

MARCH 1954

Materials Laboratory  
Contract No. AF 33(038)-20840  
RDO No. 614-16

Wright Air Development Center  
Air Research and Development Command  
United States Air Force  
Wright-Patterson Air Force Base, Ohio

## FOREWARD

This report was prepared by the University of Minnesota, under USAF Contract No. AF 33(038)-20840. The contract was initiated under Research and Development Order No. 614-16, "Fatigue Properties of Structural Materials," and was administered under the direction of the Materials Laboratory Directorate of Research, Wright Air Development Center, with Captain R. A. Tondreau acting as project engineer.

The following personnel of the University of Minnesota contributed significantly to this work: L. J. Demer, C. E. Johanson, G. G. Chapin, and J. H. Klumpp.

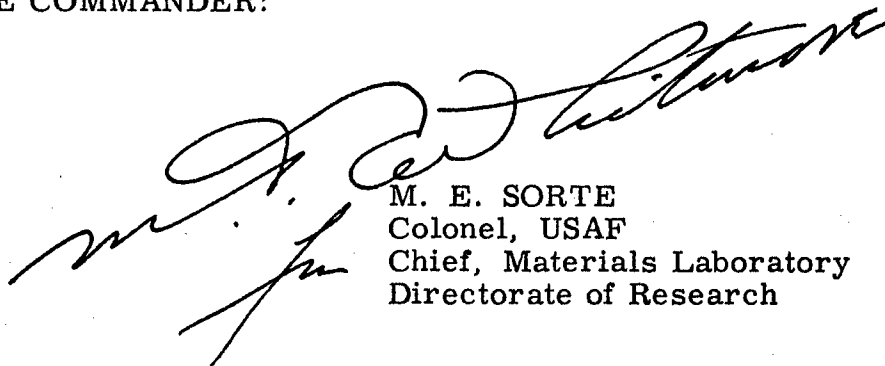
## ABSTRACT

The nature of resonant vibration and the accompanying amplification of fatigue stress are discussed in relationship to the damping energy absorbed by a vibrating system. The resonance amplification factor is defined as a measure of the severity of a resonant condition. The sources of damping in a vibrating system are discussed and classified according to whether they are external (structural) or internal (material). Data on the internal damping properties of a variety of structural materials are presented and the generalized behavior is discussed. In cases where internal damping is significant, the importance of both fatigue strength and damping properties of materials as joint criteria for resonant strength is demonstrated and quantitatively expressed. The analyses are made in terms of the resonant strength constant for the material (the material factor) and the volume-stress function of the part (the part factor).

## PUBLICATION REVIEW

This report has been reviewed and is approved.

FOR THE COMMANDER:



M. E. SORTE  
Colonel, USAF  
Chief, Materials Laboratory  
Directorate of Research

## TABLE OF CONTENTS

Section	Page
I Introduction . . . . .	1
II Nature of Resonance and Its Accompanying Amplification of Fatigue Stress . . . . .	2
III Sources of Damping in a Vibrating System . . . . .	3
3.1 External Damping With Special Reference to Slip Damping . . . . .	3
3.2 Internal Damping With Special Reference to Stress-Strain Hysteresis . . . . .	6
3.3 Comparison of Relative Magnitude of External and Internal Damping . . . . .	11
IV Fatigue and Damping Properties as Joint Criteria for Material Selection and Engineering Design for Resonant Strength . . . . .	12
4.1 Uniform Stress Distribution . . . . .	13
4.2 Non-Uniform Stress Distribution . . . . .	15
4.3 An Example . . . . .	21
V Summary and Conclusions . . . . .	21
Bibliography . . . . .	23
Appendix A - Definitions of Terms and Symbols . . . . .	24

## LIST OF TABLES

Table	Page
I Source, Chemical Composition, Production, Heat Treatment And Specimen Size of Test Materials . . . . .	27
II Damping, Elasticity, Fatigue, and Static Properties of Various Structural Materials . . . . .	29
III Effect of Heat Treatment on Properties of An Alloy Steel Part at Resonance, Both as a Material (or Uniform-Stress Part) and a Part Having High $K_v$ . . . . .	31

## LIST OF ILLUSTRATIONS

Figure		Page
1	Effect of Damping on Amplitude of Near-Resonance Vibration . . . . .	32
2	Resonance Curves for a Bolted Connection, Indicating Effect of Bolt Clamping Force . . . . .	33
3	Effect of Joint Bolt Pressure on Resonance Amplification Factor. . . . .	34
4	Typical Stress-Strain Hysteresis Loop for Material Under Reversed Axial Stress . . . . .	35
5	Comparison of the Effect of Sustained Cyclic Stress of Several Magnitudes on the Total Damping Energy of Various Materials . . . . .	36
6	Specific Damping Energy as a Function of Amplitude of Reversed Stress for Glass Laminate, Magnesium, Aluminum (24S-T4), Gray Iron, 1020 Steel, Sandvik Steel (N), and Sandvik Steel (Q-T) . . . . .	37
7	Specific Damping Energy as a Function of Amplitude of Reversed Stress for Titanium (RC55 Annealed, RC55 Cold-Worked, and RC130B) at 600° F and Room Temperature. . . . .	38
8	Specific Damping Energy as a Function of Amplitude of Reversed Stress for Type 403 at Room Temperature, N-155 at Room Temperature, 1350°, and 1500° F, and Stellite 31 As Cast at 1200°, 1350°, and 1500° F . . . . .	39
9	Dependence of Specific Damping Energy of Various Structural Materials Upon Ratio of Cyclic Stress to Fatigue Strength. . . . .	40
10	Damping Energy of Various Structural Materials at Stresses and Strains in the Engineering Range. . . . .	41
11	Specific Damping Energy at Various Ratios of Cyclic Stress to Fatigue Strength for Various Structural Materials . . . . .	42
12	Simplified Comparison of the Contributions of External and Internal Damping to a Vibrating System . . . . .	43
13	Damping-Stress Curves for Sandvik Alloy Steel, Normalized Showing Resonance Amplification Factor and Exciting Stress Grids. . . . .	44
14	Exciting Stress Required to Produce an Excited Stress Near the Fatigue Strength for Several Structural Materials Under Uniform Stress. . . . .	45
15	Graphical Method for Determining the Volume-Stress Factor $K_v$ for a Part Having Complicated Stress Distribution . . . . .	46
16	Volume-Stress Functions for Various Types of Members. . . . .	47
17	Effect of Damping Exponent $n$ on Longitudinal Stress Distribution Factor and Cross-Sectional Shape Factor of Selected Examples. . . . .	48
18	Effect of Damping Exponent $n$ on Volume-Stress Factor of Various Types of Parts . . . . .	49

## SECTION I. INTRODUCTION

Experience shows that one of the more common causes of service failure under dynamic force is near-resonant vibrations. The very serious amplification in vibration caused by the resonance, several hundred times in some cases, frequently results in dangerously large fatigue stress. It is thus apparent that in many applications it is not only necessary to investigate the fatigue resisting properties of materials and parts under known excited stress, but also the ability of such parts to withstand known exciting force at resonance.

Considerable work has been done on the fatigue and other properties of materials which define their ability to withstand specified excited cyclic stress produced by either resonant or other vibrations. However, comparatively little has been done on the analysis of the properties of materials and other factors which determine their ability to withstand specified resonance exciting force. The amplification in vibration that is caused by resonance has not received its due attention. Consequently, this paper is concerned not with fatigue alone, but with both fatigue and damping capacity as joint criteria for defining the ability of a part to withstand resonant vibrations.

There has been some service experience to indicate that fatigue strength alone does not provide a sole basis for judging materials, parts, or structures exposed to resonant vibrations. For example, under the resonant vibrations excited by wind, a copper overhead cable of relatively low tensile and fatigue strengths but high damping capacity may be more durable than a light high-strength alloy having lower damping capacity (1)<sup>1/</sup>. However, it should be emphasized that, in general, the interpretation of service experience to indicate the relative importance of the damping and fatigue properties is extremely difficult. Such factors as notch effects, surface inhomogeneity of parts, environmental unknowns, and stress distribution usually make interpretation of results inconclusive. Thus, broad generalizations regarding the relative importance of damping, both material and structural, and fatigue strength are difficult to make at this time. Nevertheless, there is little doubt that in many and diverse applications damping is of critical importance.

---

<sup>1/</sup> Numbers in parentheses refer to references in the Bibliography.

## SECTION II. NATURE OF RESONANCE AND ITS ACCOMPANYING AMPLIFICATION OF FATIGUE STRESS

Figure 1 illustrates the well-known resonance curve (2) for a simple linear system having a single degree of freedom and excited by a force of constant magnitude but variable frequency. The single degree of freedom system having the mass, spring, and damping components shown in the figure is used for simplicity of explanation. In many actual parts, two or three of these components may be combined in one member. For example, in a simple vibrating cantilever beam, the material of which the beam is made may furnish all three elements: the mass, the elasticity, and the damping. In other cases the vibrating system may have several different masses, springs, or sources of damping. However, the general observations to be made for the simple system shown in this figure usually apply to complicated multi-degree of freedom systems.

Figure 1 shows that an increase in frequency causes a gradual increase in amplitude of vibration, a peak being reached at the point of resonance where the frequency of the exciting force equals the natural frequency of the vibrating system<sup>1/</sup>. Beyond this resonance point the amplitude decreases with increasing frequencies in the region above resonance. In order to indicate the effect of magnitude of system damping, two different resonance curves are shown. The upper curve, labeled "1", with the sharpest resonance peak is characteristic of the behavior of a system with relatively low damping. If the damping is large, then the lower curve, labeled "2", illustrates the relatively flat behavior in the resonance region. It is thus apparent that the magnitude of system damping is an important factor in defining the severity of a resonant condition.

Quantitatively, the severity of a resonant vibration may be specified in terms of the resonance amplification factor. This is by definition the ratio of the excited amplitude,  $A_d$  in Figure 1, induced by an exciting force exactly at resonance to the amplitude or displacement  $A_g$  caused by the same magnitude of force applied statically or at very low frequencies. Since in the two cases covered by Figure 1 the magnitude of exciting force is assumed constant, static amplitude  $A_g$  is the same for both cases. Thus, for the two curves

---

<sup>1/</sup> There are several definitions of "resonance". For systems with large nonlinearity and extremely large damping, the definition used may have a significant effect on the results. However, for most engineering cases the rather loose definition given above is adequate.

shown, the resonance amplification factor is  $\frac{1}{\zeta}$ :

$$A_{r1} = \frac{A_{d1}}{A_g} \quad \text{for the low damping case.}$$

$$A_{r2} = \frac{A_{d2}}{A_g} \quad \text{for the high damping case.}$$

Since  $A_r$  is a reciprocal function of the damping capacity of a system, the ability of the vibrating system to absorb energy is of critical importance in defining the vibration amplitudes at a resonance.

The magnitude of the resonance amplification factor varies over a wide range. In laboratory tests, resonance amplification factors exceeding a thousand have been observed whereas in other cases values as low as one have been approached. Recent tests on a large airplane propeller, for example, revealed a resonance amplification factor of 480 (3) whereas tests of parts with large structural damping indicated resonance amplifications approaching 10 (4). Thus, the use of average values for  $A_r$  is to be discouraged; in view of the wide range of values possible each case must be considered individually.

### SECTION III. SOURCES OF DAMPING IN A VIBRATING SYSTEM

In view of the importance of total system damping in defining the severity of a resonant condition, it is desirable to review briefly the various ways in which a system can absorb vibrational energy and dissipate it as heat. For convenience in discussion, the various types of damping are classified as either (a) external (structural) or (b) internal (material) damping. Each of these two types is discussed below.

#### 3.1 External Damping With Special Reference to Slip Damping

External dampers, as discussed here, refer to energy absorbers only. Thus, energy transferring devices, seismic connections, etc. are not included in this discussion.

---

$\frac{1}{\zeta}$  See Appendix A for definition of symbols used.

In many applications, separate damping units are frequently added to reduce resonant vibrations. In vehicle suspensions, for example, dash-pot type units have been found very successful. In general, when the design is such that damping units may be attached at effective points, where there is sufficient relative motion to make them operative, separate dampers provide a suitable approach. However, additional units in the form of dampers means additional complexity and maintenance. Furthermore, in many applications (turbine blades, for example), it is extremely difficult to add extra damper units. Thus, other sources of damping must be relied upon.

Aerodynamic and other fluid effects may also provide significant damping in some cases. However, only in rather special cases does this become sufficiently large to affect significantly the amplitude of vibration at resonance.

There is, however, one form of structural damping which can be utilized in many and diverse designs. This is what might be termed slip or connection damping. In structures containing joints, significant slip may occur at mating surfaces and the accompanying friction force frequently enables the dissipation of considerable damping energy. This combination of frictional force and motion, that is, the slip-damping effect, may pronouncedly affect the resonance amplification factor as discussed below.

Tests at resonance have been made (4) on the joint shown in Figure 3. Under the bending vibrations excited by force  $F_g$  a distribution of frictional slip occurs on contact surfaces AB and CD. These surfaces provide a source of energy dissipation which can effectively limit the severity of the resonant condition as shown in Figure 2. Both the magnitude of the frictional force and frictional slip depend on several test conditions, such as magnitude of exciting force, bolt tightness, slip surface material and its condition, and lubrication. The effect of bolt pressure only is illustrated in Figure 2. Under zero bolt pressure there is relatively high amplification. As bolt pressure is increased to 25 pounds, the resonance severity is greatly reduced. However, as the bolt pressure is increased beyond 25 pounds, the resonance amplification undergoes pronounced increase.

This effect of bolt pressure on resonance amplification factor is illustrated in Figure 3 for a joint under constant excited force. The  $A_r$  trends shown in this figure are reasonable when it is considered that the energy absorbed is proportional to the product of an effective shearing force and an effective shearing motion (or slip) at the mating surfaces. When the normal pressure is extremely large, the shearing force required to produce motion is correspondingly large, and the externally applied force may be insufficient to produce significant shearing slip. Thus the product of the effective shearing force and slip may be very small. Similarly at small bolt pressures the normal and shearing force is small and thus the energy absorbed is small even though the magnitude of slip may be large. At some

optimum normal force, however, both significant shearing force and shearing slip may occur, resulting in a product which is maximum. In this region of maximum energy absorption  $A_r$  will be a minimum. Thus, the  $A_r$  pattern shown on Figure 3, maximum at very low and high bolt pressures and minimum in an intermediate region is reasonable.

Referring to Figure 3, since the joint with 50 pounds bolt force has a resonance amplification factor approximately one-sixth of that with a 1200 pound bolt force, it requires six times the exciting force to produce the same excited force. Thus, even though the 50 pound joint may be weaker in fatigue than the 1200 pound joint, it still may be considerably more durable under fatigue-producing resonant vibrations. This concept will be demonstrated later in connection with hysteresis damping of material.

Attempts have been made to analyse various specific types of joints, for example, turbine blade connections (5). However, discussion of this is beyond the scope of this paper.

In many cases it is desirable for ease in comparison, computation, and analysis to lump all external damping together and specify them in terms of equivalent viscous damping constants (6). This permits study of the resonance phenomena by the use of rather simple constants even though the sources of damping may be many and rather complicated. Under these conditions damping is usually assumed to vary as the square of the amplitude.

In other cases of external damping, however, the assumption that damping energy increases with the square of amplitude is not accurate. For example, several different damping relationships are possible in joints having slip damping only. If the joint is so constructed that the relative motion at all points of contact is equal, such as would occur if the joint shown in Figure 3 were vibrated axially, then damping increases linearly with amplitude. However, if the same joint is subjected to reversed bending as indicated in Figure 3, then damping energy increases with the cube of the vibration amplitude. In other types of joints of the same type (for example, if the internal part ABCD were tapered), the slip distribution may be such as to result in still another relationship. Thus, in slip-type structural damping various exponents from 1 to 3 have been observed and a wider range of values is likely.

The power function also appears to describe other types of external damping. If air friction is the primary cause of damping, for example, then the damping energy usually varies as a cube of amplitude.

For convenience in comparing external and internal damping it is desirable to express damping in terms of maximum stress  $S_c$  in the part. In general, it may be assumed with reasonable accuracy that the stress in the part is proportional to the amplitude<sup>1/</sup>.

---

<sup>1/</sup>The error in this assumption depends on how much the dynamic modulus of the material or stiffness of the structure varies with stress and stress history. However, this variation can generally be considered small.

Thus, the total structural or external damping  $D_x$  in a part may be written as:

$$D_x = J S^n \quad (1)$$

The damping exponent  $n$  varies from 1 to 3 for many cases of slip damping, equals 2 for viscous damping, and equals 3 for air friction damping.

### 3.2 Internal Damping With Special Reference to Stress-Strain Hysteresis

The stress-strain curve for a material subjected to vibratory stress is shown in Figure 4. For simplicity it is assumed that the specimen vibrates between equal limits of tension and compression under completely reversed stress. Due to hysteresis effects in the material, the unloading branch AB of the stress cycle falls to the right of the initial loading branch OEA (curves OEA and AB coincide only for perfect elastic materials). The permanent set OB, which remains after stress cycle OAB, is a measure of the inelasticity in the material up to stress  $S_t$ .

The damping capacity of a material depends on the net energy absorbed by the material during a stress cycle. It is therefore proportional to the area within the hysteresis loop ABCDA. This area generally increases with increasing amplitude of stress  $S_t$ , sometimes very rapidly as discussed later.

Experimental data indicate that no material displays zero damping capacity however small the stress cycle may be. Thus, no material is perfectly elastic even at very low stresses. It therefore follows that no material exactly obeys Hooke's Law of proportionality between stress and strain under alternating force.

Damping energy is also a measure of the internal heat generated in the material under cyclic stress. Thus, a specimen or part under cyclic stress will increase in temperature until the heat loss from the specimen to the environment equals the energy represented by its damping capacity. Thus, materials sometimes increase significantly in temperature during the course of a fatigue test. This, incidentally, may sometimes be an important factor in understanding fatigue failure, particularly at higher frequency.

The inelastic behavior of materials as evidenced by internal heating does not always indicate impending failure. One fatigue test (1), for example, was continued for over three years during which period there was sufficient inelastic behavior or damping in the specimen to maintain its temperature above 270° F. Nevertheless, after a billion stress cycles the specimen showed no signs of failure. Hysteresis damping should not, therefore, always be associated with weakness or impending fatigue failure in the material. However,

excessive heating in a fatigue specimen frequently does occur in tests above the fatigue limit.

Before discussing the relationship between damping and the severity of a resonant vibration, it is desirable to first review the effect of stress and stress history on damping energy. In order to do so in a basic way the damping properties determined in this work are presented in terms of specific damping energy. This provides not only a fundamental unit of measurement but also is convenient in analysing the engineering significance of damping (9).

It should be emphasized that the specific damping unit used in this paper may be quite different from the average damping energy sometimes used in prior work. The specific damping energy is the unit value associated with a specific stress or that which would be observed if the entire specimen were under uniform stress distribution, such as occurs in axial tension-compression. It therefore does not depend on specimen shape and stress distribution. The average damping, on the other hand, depends not only on material but also the stress distribution in the test specimen (7). The comparison and use of average damping data therefore becomes rather difficult.

Since the difference between the average and specific damping may be large in some cases, it is desirable to determine this effect quantitatively. To do so consider first the absolute energy expressions for the total damping of a test specimen.

$$D_o = \int D dV = \int D \frac{dV}{dS} dS \quad (2)$$

Now if  $D_a$  is defined as the average damping energy for stresses from 0 to  $S_1$ , and  $D_1$  is defined as the specific damping energy associated with stress  $S_1$ , then:

$$D_a = \frac{D_o}{V_o} = \frac{D_1}{V_o} \int \frac{D}{D_1} \frac{dV}{dS} dS \quad (3)$$

and

$$T = \frac{D_1}{D_a} = V_o / \int \frac{D}{D_1} \frac{dV}{dS} dS \quad (4)$$

It can be shown from Equation (4) that for structural materials the average damping  $D_a$  equals the specific damping  $D_1$  (that is,  $T = 1$ ) only under uniform stress distribution. Under bending stress the ratio  $T$  may be considerably larger than one, being larger even than 10 for many types of damping and stress distribution functions. For example, if:

- (a)  $D/D_1$  is a power function of stress (which is shown later to be reasonable over certain ranges of stress), and
- (b) the specimen is a rotating beam (which has a stress distribution such that  $dV/dS = 2 V_0 S/S_1$ ), then

$$T = \frac{n+2}{2} \quad (5)$$

Thus, if damping exponent  $n=2$ , then  $T=2$ , and if  $n=6$  then  $T=4$ . For parts like a vibrating cantilever beam having rectangular cross-section and linearly increasing moment from the tip (which approximates a tuning fork sometimes used in damping work) the stress distribution is less favorable. Under these circumstances  $T=(n+1)^2$ ; thus,  $T=9$  for  $n=2$  and  $T=49$  for  $n=6$ .

If damping is expressed in terms of logarithmic decrement or other unit involving the ratio between damping energy and elastic energy, a difference between average and specific values can also be demonstrated. In the case of energy ratio units, no error occurs if damping exponent  $n=2$  (since the elastic energy also increases with the square of stress). But if the damping exponent is 6, for example, the logarithmic decrement of the vibrating cantilever mentioned above will be only one-fifth of that of a vibrating axial stress member (uniform stress distribution) made of the same material and operating in the same stress range.

It is thus apparent that specific units of damping rather than average units should be used in analyses. Furthermore, if average units are used in studying the damping phenomena, "low stress over large volume" effects may so camouflage "high stress over small volume" effects that significant high stress trends may be entirely missed. This may be the primary reason why in earlier work some of the characteristics of the damping curves discussed in this paper were not generally observed.

Damping, elasticity, and fatigue data were procured on a variety of structural materials for which the composition, general properties, etc. are given in Tables I and II. The type of damping data determined directly from rotating beam testing (15) are illustrated in Figure 5. These data were procured during the course of conventional (constant stress amplitude) fatigue tests. Observe first that at relatively low stress, damping does not change with stress history (that is, number of stress cycles) but as the stress approaches the fatigue limit damping is affected by repeated fatigue stress. Many different patterns of change have been observed under sustained cyclic stress. Mild steel and Sandvik steel (quenched and tempered) display increasing damping with increasing number of stress cycles as shown

in Figure 5. However, 24S-T4 aluminum shows reductions in damping. Normalized Sandvik steel and J-1 magnesium display both increases and decreases under sustained vibrations, depending on stress level and history.

The type of data given in Figure 5 may be replotted as shown in Figures 6, 7, and 8 to show damping versus stress amplitude on a log-log basis. Stress history effects in the high stress region are shown in these figures by means of a family of curves for each material. For example, the curve labeled "1.3" in the 1020 steel family indicates the damping energy after  $10^{1.3}$  or 20 cycles, and the curve labeled "6" after  $10^6$  or one million cycles.

The series of curves shown in Figures 6, 7, and 8 reveal several points of similarity. First of all each curve (except that for the glass laminate) has a "cyclic stress sensitivity limit" (see solid square dots in figure) below which the curve showing log damping versus log stress is a straight line (except for type 403 alloy) displaying no stress history effect. However, above this CSSL point, two changes occur. First, in all metals the damping becomes not only a function of stress amplitude but also of number of prior stress cycles, and thus a separate curve is required for each stress history. Secondly, a change in slope of the curve occurs, in some cases quite abruptly (for example, see Sandvik steel). In almost all cases, the CSSL point falls a little below the fatigue strength of the material.

Since the log damping versus log stress is a straight line below the cyclic stress sensitivity limit (CSSL) point for most materials<sup>1/</sup>, the following equation may be used to represent damping as a function of stress in the low stress region (say up to very approximately 80 per cent of the fatigue strength):

$$D = J S^n \quad (6)$$

For the materials diagrammed, the slope or value of exponent  $n$  varies between two and three in the low stress region.

Above the CSSL point, the relationship is not quite as simple. In this region slope  $n$  of the curve may increase abruptly, values exceeding 20 having been observed in several cases. The significance of the rapid increase in damping as a limiter of resonant vibrations is discussed later.

---

<sup>1/</sup>This is not true for materials which display large magneto-mechanical effects (10). For example, the curve for type 403 alloy shown in Figure 8 shows considerable curvature.

In order to aid in explaining the engineering significance of damping energy and to reveal more clearly the trends in hysteresis damping, Figures 6, 7, and 8 are replotted in Figure 9 using as the abscissa the ratio of cyclic stress to fatigue strength  $S_e$ . In order to avoid confusion, all the damping curves are not drawn in this diagram; in most cases only the extremes (see small circles) and the cyclic stress sensitivity limit (see small squares) are shown. Observe that even though the several structural materials shown cover a wide range of materials and temperatures; the following general observation can be made:

- (a) With very few exceptions the data fall within the shaded band shown. The only material which is seriously outside the shaded band is type 403 alloy at low stress, a material with large magneto-structive damping (10) and a curved low-stress damping line. Also Stellite at 1350° and 1500° F at low stress may lie above the shaded band.
- (b) The cyclic stress sensitivity limits occur at ratios of stress to fatigue strength having an extreme spread from 0.33 to 1.06. However, all but four materials fall in the 0.45 to 0.94 range. The approximate average location of the CSSL for all materials studied is at a ratio of 0.8.

In view of the above observations, it is possible to establish within the shaded band a "geometric mean" curve shown in Figure 9. For convenience, the "mean" curve was made to pass through a damping value of 1 in-lb per cu in per cycle at its CSSL (ratio of 0.8). Below this value, damping decreases with the 2.4 power of stress and above this value it increases as the 8.0 power of stress. Thus, the equation for the "geometric mean" curve is:

$$D = 1.7 \left( \frac{S}{S_e} \right)^{2.4} \quad \text{for } S/S_e < 0.8 \quad (7)$$

$$D = 6.0 \left( \frac{S}{S_e} \right)^8 \quad \text{for } S/S_e > 0.8$$

The scatter in damping about this "geometric mean" curve (as indicated by the shaded area in Figure 9) is such that the different materials included in this plot may have the following approximate range of values: from 1/3 to 3 times the "mean" values at a stress ratio of 0.2 or less, from 1/5 to 5 times at a ratio of 0.6, from 1/10 to 10 times

at a ratio 1.0, and 1/50 to 50 times the average at a ratio of 1.2.

In material selection and other design problems, a comparison of the damping properties of various materials is sometimes necessary. Such a comparison is attempted in Figures 10 and 11.

The specific damping energy of various structural materials at stresses and strains of engineering interest are shown in Figure 10. The stresses in thousands of psi are given by the boxes on the left of each column and the unit strains in thousandths of an inch per inch are indicated on the right. The cyclic stress sensitivity limit and fatigue strength of each material is indicated by the  $L$  and  $S_e$  symbols.

Although in some material selection and engineering design problems comparisons on a basis of unit stress or unit strain are required, this is not true in most problems involving the strength of a part at resonance. In resonant strength analyses, comparisons on a basis of ratio of cyclic stress to fatigue strength becomes more significant (see Equations 14 and 17). This basis of comparison is shown in Figure 11, which presents a relative rating for the various materials quite different from that shown in Figure 10.

An extensive discussion of relative merits of the various methods of comparison is beyond the scope of this paper. This subject is briefly discussed in Reference (15).

It is somewhat revealing to convert damping energy  $D$  to horsepower. The range of damping at the fatigue limit is 0.5 to 100 in-lb per cu-in per cycle. At 3600 cycles per minute, a material with a damping of 100 would absorb one horsepower for each cubic inch under uniform stress at the fatigue limit (assuming damping is frequency insensitive).

Internal damping may also be caused by effects other than stress-strain hysteresis. These include eddy current and magnetic effects. However, since these have rather limited structural applicability and are generally relatively small in magnitude, they are not discussed in this paper.

### 3.3 Comparison of Relative Magnitude of External and Internal Damping

There are insufficient data and analyses to generalize regarding the relative importance of internal damping and external damping as limiters of resonant vibration. It is generally believed, although there is practically no substantiating data, that external damping is larger than internal damping in almost all engineering cases. Blind acceptance of this generalization should be discouraged since in some systems there is little opportunity for structure damping and internal hysteresis is the only source of significant energy absorption. Furthermore, even in cases where there is considerable external damping, large internal damping may still be very helpful in limiting high stress resonant vibrations as discussed below.

An attempt is made in Figure 12 to illustrate a comparison between total external and internal damping. As discussed previously, it is possible in many cases to lump all external damping together and represent it by a single damping relationship. Although the external damping exponent may vary over a wide range (that is  $n = 1$  to  $3+$ ), for illustrative purposes, it is assumed that as an average external damping increases as a 2.4 power of amplitude or stress. Also for illustrative purposes the "geometric mean" curve shown in Figure 9 is assumed to be representative of material damping. Furthermore, it is assumed that the stress distribution in the part (which is discussed later) is favorable so that the total damping curve for the material is similar to the specific damping curve. The external and internal damping curves based on these assumptions are compared in Figure 12.

Assume now that, as an extreme case, the external damping is much larger than the internal damping (Case A of Figure 12). In this case even if the very substantial increase in internal damping which occurs above the CSSL is considered, the material damping still does not offer a significant contribution to the total damping until the stress gets dangerously above the fatigue limit. Consider next Case B which is probably representative of many engineering applications. At low stress levels external damping predominates. However, above the CSSL and as the fatigue strength is approached the internal damping may begin to assume importance and even dominate. Furthermore, at high stress, such as might occur during transient overloading, the material damping may build up extremely rapidly and serve as an effective safety valve in limiting resonant vibrations. In many applications, dangerously high resonant stresses may occur for relatively few cycles either during known transient conditions or unexpected overloadings. Thus, the rapid increase in damping properties near and above the fatigue strength is of considerable engineering importance.

In Case C the internal damping is above the external damping over the entire range of stress. This is probably the least common of the three cases.

#### SECTION IV. FATIGUE AND DAMPING PROPERTIES AS JOINT CRITERIA FOR MATERIAL SELECTION AND ENGINEERING DESIGN FOR RESONANT STRENGTH

As discussed previously, both external (structural) damping and internal (material) damping combine in most applications to limit the severity of resonant vibrations. In view of the varieties of types and magnitudes of external damping encountered, it is extremely difficult to classify and generalize until considerably more basic work is done in this field. In the case of material damping, however, some generalizations are possible. Thus, an

attempt is made below to clarify the damping and resonant strength properties of parts in which the material hysteresis damping is the primary source of energy absorption (see Case C of Figure 12). Attempts to extend this treatment to include structural damping must await additional work.

Damping affects both the shape of a resonance curve and its peak values. In engineering problems involving fatigue failure, the peak or maximum force is of primary concern. Thus, in this paper only the effect of damping energy on the resonance amplification factor  $A_r$  is considered. For most applications, in which sinusoidal motion may be assumed with reasonable accuracy, this factor may be computed from the following equation:

$$A_r = 2\pi \frac{W_o}{D_o} \quad (8)$$

Equation (8) shall now be used to compute the resonance amplification of different types of members.

#### 4.1 Uniform Stress Distribution

Before treating the general case of a part having a non-uniform stress distribution, it is desirable first to discuss the greatly simplified case of uniform stress distribution such as occurs in an axially loaded member (tension-compression). For this special case  $W_o = V_o S_d^2 / 2E$ , thus:

$$A_r = \pi S_d^2 / ED \quad (9)$$

If the difference between the static and dynamic modulus of elasticity may be assumed to be small in comparison with the stress differences under consideration, which is a reasonable assumption in most cases of resonant vibrations<sup>1/</sup>, then:

$$A_r = \frac{S_d}{S_g} \quad (10)$$

---

<sup>1/</sup> Assumptions regarding constancy of the shape of the elastic curve must also be made under certain conditions.

and

$$S_g = \frac{S_d}{A_r} = \frac{ED}{\pi S_d} \quad (11)$$

Before discussing the significance of resonance exciting stress  $S_g$ , it is desirable to first diagram the relationship given by equations (9) and (11) and illustrate how both the resonance amplification  $A_r$  and exciting stress  $S_g$  vary under uniform stress distribution for a rather typical damping curve. For this purpose the Sandvik steel curves shown in Figure 6 are reproduced in Figure 13. Added to this figure to show important trends are  $A_r$  and  $S_g$  grid lines, computed from equations (9) and (11). Since for constant  $E$ , these values are functions of  $D$  and  $S_d$  only, the grid lines are independent of the damping curve of the material (although for clarity the grid is drawn in the vicinity of the damping curve only).

In the region below the cyclic stress sensitivity limit, where  $n = 2.5$ ,  $A_r$  decreases rather slowly with increasing stress, from approximately 700 at 10,000 psi to approximately 220 at the CSSL of 52,000 psi. In this same region the resonance exciting stress  $S_g$  is extremely low, increasing from about 17 psi at 10,000 psi excited stress to about 250 psi at the CSSL. However, above the CSSL the damping curves take a pronounced upward swing and display an average slope  $n$  of approximately 20. Correspondingly,  $A_r$  decreases rapidly and  $S_g$  increases rapidly as shown, so much so that at 130 per cent of fatigue strength  $A_r$  equals 3 and  $S_g$  equals 35,000 psi.

In view of the above, it becomes apparent that the criteria for resonance strength is not fatigue strength alone, but some combination of fatigue strength and damping capacity. The relative importance of each of these properties depends on a number of factors which shall be discussed later. However, confining the present discussion to the case of uniform stress distribution, such as occurs in tension-compression members, it is possible to rate the relative ability of materials to resist resonant vibrations. This can be done in terms of their ability to withstand exciting stress  $S_g$  which will cause an excited stress  $S_d$  equal to the fatigue strength  $S_e$ . Defining this exciting stress as  $S_{ge}$  the resonance amplification factor at this stress is:

$$A_{re} = \frac{S_e}{S_{ge}}$$

and

$$S_{ge} = \frac{E D_e}{\pi S_e} \quad (12)$$

The term  $S_{ge}$  may be defined as the resonant strength constant of the material and is seen to depend not only on fatigue strength ( $S_e$ ) but also damping properties at the fatigue strength and the modulus of elasticity. Damping at the fatigue strength may vary considerably with stress history; for example, for the steel shown in Figure 13  $A_{re}$  decreases from 60 to 9 and  $S_{ge}$  increases from 1,400 to 8,000 psi with increasing stress history.

It will be shown later that the resonant strength constant of the material is merely one of several factors which define the resonant strength of a part. However, at this point it may be stated that if either:

- (a) a part is exposed to a uniform stress distribution, or
- (b) the damping exponent  $n = 2$ ,

then the resonant strength constant of the material is a direct measure of the resonant strength of the part. Under these conditions it specifies the allowable exciting stress  $S_{ge}$  in psi, which the part can withstand without exceeding the fatigue limit.

Table II and Figure 14 present a comparison of the resonant strength constants for several widely different structural materials. It is interesting to note that there appears to be no correlation between fatigue strength and the resonant strength constants. Observe also that the resonant strength constants cover a considerably wider range of values than the fatigue strengths. Although for the materials indicated,  $S_{ge}$  covers a range of 10-1,  $S_g$  for 60 per cent  $S_e$  covers a range of 33-1,  $S_g$  for 100 per cent  $S_e$  covers a range of 230-1, and  $S_g$  for 120 per cent  $S_e$  a range of 330-1. Furthermore, the material with the highest  $S_g$  for 60 per cent  $S_e$  is Gray Iron, the weakest of the group; whereas, normalized Sandvik steel, RC-55 Titanium, N-155, and mild steel, which are scattered in various positions within the fatigue strength rating have the highest  $S_g$  values for 100 per cent and 120 per cent  $S_e$ .

#### 4.2 Non-Uniform Stress Distribution

The primary concern up to this point has been with the basic damping and fatigue properties of materials and their interpretation in terms of the behavior of a resonant member

under uniform stress distribution only. In practice this rather desirable state of uniform stress is quite rare. Almost always, critical members are stressed non-uniformly, in which case equations (9) and (11) do not hold. Therefore, in the interest of providing wider engineering applicability for the type of damping data presented, an analysis of the resonance amplification factor  $A_r$  for parts having non-uniform stress shall be presented.

Marin and Stulen (11) have analysed a cantilever beam from this viewpoint, assuming that damping increases as the cube of stress. A more general treatment was also attempted (10) (14) in which a variety of types of members were analysed assuming damping increases with the  $n^{\text{th}}$  power of stress. The total damping and resonance amplification of various parts have also been analysed (11) (13) utilizing an approach which involves damping-stress and volume-stress functions so that simplifying assumptions need not be made regarding the shape of the damping curve.

The summary given below integrates and slightly amplifies the publications cited above.

Applying equation (8) to the case of non-uniform stress:

$$\begin{aligned}
 A_r &= 2 \pi \frac{W_o}{D_o} = \frac{\pi}{E} \frac{\int S^2 dV}{\int D dV} \\
 &= \frac{\pi \int S^2 \frac{dV}{dS} dS}{E \int D \frac{dV}{dS} dS} \quad (13)
 \end{aligned}$$

where the term  $dV/dS$  is procured from what has been called the stress distribution function by Cochardt (10) and the volume-stress function by Lazan (12).

Extracting the resonant strength constant  $S_{ge}$  from the above equation and placing it in a dimensionless form:

$$A'_{re} = \frac{\pi S_e^2}{E D_e} \frac{\int \left(\frac{S}{S_e}\right)^2 \frac{dV}{dS} dS}{\int \frac{D}{D_e} \frac{dV}{dS} dS} \quad (14)$$

By definition, let

$$K_v = \frac{\int \left(\frac{S}{S_e}\right)^2 \frac{dV}{dS} dS}{\int \frac{D}{D_e} \frac{dV}{dS} dS} = \frac{\int \left(\frac{S}{S_e}\right)^2 \frac{d(V/V_o)}{d(S/S_e)} d(S/S_e)}{\int \frac{D}{D_e} \frac{d(V/V_o)}{d(S/S_e)} d(S/S_e)} \quad (15)$$

Therefore, from equations (12) and (14):

$$A'_{re} = K_v \frac{S_e}{S_{ge}} = K_v A_{re} \quad (16)$$

Thus the resonant strength of the part is:

$$S'_{ge} = \frac{S_e}{A'_{re}} = \frac{S_{ge}}{K_v} \quad (17)$$

The above equations show that the resonant strength  $S'_{ge}$  of a part is the quotient of the two factors:

- (a)  $S_{ge}$ , the resonant strength constant of the material of which the part is made (the material factor), and
- (b)  $K_v$ , the volume-stress factor which defines the stress distribution of the part and its implications (the part factor). The factor  $K_v$  has a value of one for parts which either have a uniform stress distribution, or are made of materials with damping proportional to stress squared. It is greater than one for parts with non-uniform stress distribution if  $D$  increases more rapidly than the square of stress, which is almost always so.

It has been shown (10) that this part factor may depend not only on the shape and stress distribution of the part but also on the shape of the damping versus stress curve. This will be discussed later by an example.

If one desires to know the exciting stress  $S_g$  required to produce an excited stress  $S_d$  other than the fatigue strength and  $A_r$  under these stress conditions, it is merely necessary to replace in the above equations  $S_e$  by  $S_d$  and  $D_e$  by  $D$  at stress  $S_d$ .

If both  $D/D_e$  and  $dV/dS$  can be expressed mathematically as a function of stress, then equation (15) may be solved directly. However, this can not always be done. Although in many cases the relationship between damping and stress may be assumed to be  $D = J S^n$  over a sufficiently wide range of stress to be useful, there are cases where magneto-mechanical damping (10) or high stress effects (8) cause serious deviations. Similarly, even though  $dV/dS$  can be easily expressed mathematically for simple cases of axial stress, bending, and torsion, the expression becomes too involved to be handled mathematically in most actual parts. Consequently, it may become necessary to use a graphical integration approach.

The graphical approach suggested by the above equations is illustrated in Figure 15 and outlined below:

- (a) Either compute or experimentally determine the stress distribution of the part in such a way that a volume-stress curve of the type shown in Figure 15a may be plotted. Volume  $V$  in this figure is that which has a stress less than the corresponding abscissa value of  $S$  and  $V_0$  is the total volume of the part for which the stress is considered significant.
- (b) Construct Figure (b) from the slopes of Figure (a). In some cases it may be easier to construct Figure (b) directly from the experimental stress distribution data and computations.
- (c) Construct Figure (e) as indicated for Figure (b). This represents the elastic energy (area  $\beta$ ).
- (d) Run damping tests and plot Figure (c), which represents the damping properties of the material at the stress history considered. It should be emphasized that this figure must be based on specific rather than average damping energy.
- (e) Combine Figures (b) and (c) as shown to produce (d). This represents the damping energy (area  $\alpha$ ).
- (f) Measure the areas of Figures (d) and (e). Compute  $K_v$  using the equations indicated. The resonance amplification factor or the resonant strength of the part may then be computed from equations (16) and (17).

Various types of volume-stress functions are shown in Figure 16, a unitless basis of comparison being used to facilitate comparison<sup>1/</sup>. In this figure curve 1 represents the

---

<sup>1/</sup> In analysing the beams the assumption was made that stress is proportional to the distance from the neutral axis. Although this is not exactly so under conditions of variable dynamic modulus of elasticity, the errors involved are considered too small to seriously affect the conclusions presented.

volume-stress function of a part having most of its volume at near peak stress, for example a tension-compression member without serious discontinuities. This type of part has a low  $K_V$  value. At the other end of the scale a part having high  $K_V$  (curve 6) would have very little of its volume at near peak stress. For example, curve 6 might be representative of a notched bar in bending. In between these two extremes lie several common types of members (curves 2, 3, and 4) and one particular type of turbine blade (curve 5). For parts made of the same material and stressed to the same maximum stress curve 1 (low  $K_V$ ) is generally indicative of small resonance amplification factor and curve 6 (high  $K_V$ ) usually implies high  $A_r$ .

In the foregoing treatment no assumptions were made regarding the nature of the variation between damping and stress. It is now desirable to determine what simplifications are possible for various assumed damping-stress functions. For the variety of materials diagrammed in Figures 6, 7, 8, and 9, it may be seen that for a given stress history the log-log damping curve may be approximated reasonably well by two straight lines with the discontinuity at or near the CSSL. Thus:

$$D \int_0^{S_L} = J S^n \quad \text{and} \quad D \int_{S_L}^{S_e} = J' S^{n'} \quad (18)$$

Thus, Equation (15) may be simplified as follows:

$$K_V = \frac{\int_0^{S_e} \left(\frac{S}{S_e}\right)^2 \frac{dV}{dS} dS}{\int_0^{S_L} \left(\frac{S}{S_e}\right)^n \frac{dV}{dS} dS + \int_{S_L}^{S_e} \left(\frac{S}{S_e}\right)^{n'} \frac{dV}{dS} dS} \quad (19)$$

The above equation may permit applicability of an analytical approach in cases for which Equation (14) would require a graphical solution. However, this equation still does not readily indicate general trends.

For many materials even more restrictive assumptions may be made regarding the damping-stress relationship. For the laminated plastic, for example, the log-log plot is a

straight line and damping is a power function of stress. For this material, therefore, the equation  $D = J S^n = 4.2 \times 10^{-12} S^{2.3}$  holds for the entire range of stress studied (up to over 150 per cent of the fatigue strength). Similarly, for cast iron the stress history effects are rather small and the same sort of power functions can be used. For still other cases the cyclic stress sensitivity limit is so close to the fatigue strength that the same assumption may be used.

Under such circumstances, the Equation (19) may be reduced as follows:

$$K_v = \frac{\int \left(\frac{S}{S_e}\right)^2 \frac{dV}{dS} dS}{\int \left(\frac{S}{S_e}\right)^n \frac{dV}{dS} dS} \quad (20)$$

For this simplified case it has been shown (10) that the part factor  $K_v$  may frequently be broken down into two separable factors. One of these is the cross-sectional shape factor  $K_c$  (which quantitatively expresses the effect of stress distribution on a cross section) and the second the longitudinal stress distribution factor  $K_s$  (which gives the effect of stress distribution along the length of the beam). Thus:

$$K_v = K_s K_c \quad (21)$$

Under these conditions it is possible to make some significant generalizations (10) regarding the pronounced effect of damping exponent "n" on each of these factors. Some of the results are shown in Figure 17 for constant cross-section beams. In general, these curves indicate that high  $K_s$  and  $K_c$  are associated with a high damping exponent  $n$ , other factors being equal. Also, as observed previously, high  $K_v$  occurs when very little material is at near peak stress (for example, compare diamond cross-section shape with I-beam or compare uniform movement beam with vibrating cantilever). These concepts are discussed in greater detail in reference (9).

Figure 18 shows  $K_v$  as a function of damping exponent  $n$  for several cases.  $K_v$  for the beams was determined from the  $K_s$  and  $K_c$  data given in Figure 17 and  $K_v$  for the turbine blade from data given in reference (14).

Since damping exponent  $n$  rarely exceeds 3 below the CSSL, it may appear that extending Figures 17 and 18 beyond this value is purely of academic interest. However,

it is sometimes possible to determine qualitatively the implications of high  $n$  above the CSSL by referring to "equivalent"  $n$ 's having a constant value over the entire stress range.

### 4.3 An Example

In order to clarify some of the concepts presented and indicate the significance of the various terms and properties, a sample calculation is discussed below.

The fundamental damping and fatigue properties of Sandvik steel in two conditions of heat treatment are presented in Figures 5, 6, 9, and 13 and Table II. If one is concerned only with the resonant strength of these two materials and parts made from them, then only the properties listed in the last few rows of Table III need be considered. Observe that even though the normalization treatment reduced the fatigue strength 17 per cent it increased the damping energy  $D_e$  at the fatigue strength by 3000 per cent. This large increase in damping causes a corresponding decrease (from 400 to 8.9) in the resonance amplification factor  $A_{re}$  of the material (or part under uniform stress). Thus, although the fatigue strength of the quenched and tempered steel is significantly higher than the normalized steel, its resonant strength constant  $S_{ge}$  is considerably lower (230 psi compared with 8550 psi).

In order to illustrate how these properties affect the behavior of a part having a sharply increasing volume-stress function (high  $K_v$ ) the turbine blade data plotted as curve 5 in Figure 16 is used. The  $K_v$  values under these conditions, computed by using the graphical approach illustrated in Figure 15, are given in Table III. Since  $K_v$  depends not only on the volume-stress function of the material but also the shape of the damping-stress curve, it is quite different for the two materials. The normalized steel has a much higher  $K_v$  because its damping versus stress curve increases sharply as the stress approaches the fatigue strength. This results in a much higher  $D_e$  and a corresponding smaller  $D/D_e$  term (see Equation 15). Referring to the last two rows of Table III it is observed that even as a part with a sharply increasing volume-stress function, the normalized steel has lower resonance amplification factor  $A'_{re}$  (200 compared to 500) and thus a larger resonant strength  $S'_{ge}$  (380 psi compared to 160 psi).

## SECTION V. SUMMARY AND CONCLUSIONS

The increasing importance of resonance as a cause for fatigue failure is discussed. The nature of resonant vibration and its accompanying amplification of fatigue stress are demonstrated with the aim of illustrating the significance of system damping. The term resonance amplification factor  $A_r$  is introduced and defined as a measure of the severity

of resonance.

The sources of damping in a vibration system are classified according to whether they are external (structural) or internal (material) in nature. The manner in which each of these types of damping build up with stress is discussed.

Basic damping, elasticity, and fatigue data are presented for a variety of structural material materials at several testing temperatures. Several generalizations are made with regard to the existence of a cyclic stress sensitivity limit and the general damping patterns on both sides of this limit. These trends are discussed in terms of a "geometric mean" damping curve and scatter about this curve. It is shown that generally material damping is more likely to offer significant contributions near or above the fatigue limit than at lower stress levels.

For the cases in which material damping offers significant contribution to total damping the importance of both fatigue strength and damping as joint criteria for resonant strength is demonstrated. Equation and data are presented for quantitatively evaluating resonant strength constants of materials under uniform stress distribution. These indicate a dependence of resonant strength on fatigue strength, damping energy, and dynamic modulus of elasticity. Since the range of damping properties is much larger than the range in fatigue strength for the materials investigated, the critical importance of damping becomes apparent.

The effect of non-uniform stress distribution in a part on its resonant strength is quantitatively expressed in terms of volume-stress factor  $K_V$ . Methods for determining  $K_V$  and its dependence on part shape, stress distribution, and the general form of the damping versus stress curve are discussed.

The analyses presented indicates that the resonant strength of a part is affected by:

- (a) the material factor as defined by its resonant strength constant, which involves the fatigue strength, damping properties, and modulus of elasticity of the material, and
- (b) the part factor as defined by its volume-stress factor  $K_V$ .

It is shown that if internal damping is significant, the fatigue strength alone of a material is not, in general, a good indication of its resonant strength as a part. In fact, for high resonant strength it may be desirable in many cases to select materials, heat treatments, etc., which produce less than highest fatigue strength but have favorable damping properties.

## BIBLIOGRAPHY

1. Foppl, O., "The Practical Importance of Damping Capacity of Metal, Especially Steels," *The Journal of the Iron and Steel Institute*, No. 2, pp. 393-455 (1936).
2. Den Hartog, J. P., "Mechanical Vibrations," McGraw-Hill (1940).
3. Private Communications with Mr. Paul Ramsey, A. O. Smith Company, Milwaukee, Wisconsin.
4. Lazan, B. J., Brown, J., Gannett, A., Kirmser, P., and Klumpp, J., "Dynamic Testing of Materials and Structures with a New Resonance Vibration Excitor and Controller," *Am. Soc. Test. Mat.*, Vol. 52 (1952).
5. Hanson, M. P., Meyer, A. G., and Manson, S. S., "A Method of Evaluating Loose-Blade Mounting, as a Means of Suppressing Turbine and Compressor Blade Vibrations," *Proc. Soc. Exptl. Stress Anal.*, Vol. X, No. 2, pp. 103-110 (1953).
6. Plunkett, R., "Vibration Damping," *Applied Mechanics Reviews*, Vol. 6, No. 7 (July 1953).
7. Demer, L. J. and Lazan, B. J., "Damping, Elasticity, and Fatigue Properties of Unnotched and Notched N-155 at Room and Elevated Temperatures," WADC Technical Report 53-70, February 1953. Also presented before *Am. Soc. Test. Mat.*, June 1953, and to be published in *Proceedings of the Society*.
8. Demer, L. J. and Lazan, B. J., "The Effect of Stress Magnitude and Stress History on the Damping, Elasticity, and Fatigue Properties of Metallic Materials," Report on ONR Contract N8-ONR-66207, Project NR-064-361 (September 1953).
9. Lazan, B. J., "Effect of Damping Constants and Stress Distribution in the Resonance Response of Members," *J. Applied Mechanics*, pp. 201-209 (June 1953).
10. Cochardt, A. W., "The Origin of Damping in High-Strength Ferromagnetic Alloys," *J. Applied Mechanics*, pp. 196-200 (June 1953).
11. Marin, J. and Stulen, F. B., "A New Fatigue Strength-Damping Criterion for the Design of Resonant Members," *J. Applied Mechanics*, pp. A-209 and A-212 (September 1947).
12. Lazan, B. J., Status Report 53-1 on "Properties of Materials and Joints Under Alternating Force," to Wright Air Development Center, February 1953.
13. Klotter, Karl, "Technische Schwingungslehre," Springer-Verlag, Berlin, Germany, 1951, pp. 237-246.
14. Cochardt, A. W., "A Method for Determining the Internal Damping of Machine Members," Paper No. 53-A-44 to be presented before Applied Mechanics Meeting in New York, December 1953.
15. Lazan, B. J. and Demer, L. J., "Damping, Elasticity, and Fatigue Properties of Temperature-Resistant Materials," *Proc. Am. Soc. Test. Mat.*, Vol. 51, (1951).

## APPENDIX A

### DEFINITION OF TERMS AND SYMBOLS

- $A_d$  = excited amplitude at resonance = amplitude of vibration at resonance produced by exciting force  $F_g$  .
- $A_g$  = exciting amplitude = deflection if force  $F_g$  were applied statically = amplitude of vibration if  $F_g$  were applied at very low frequency, well below resonance where  $A_v$  is equal to 1 .
- $A_r$  = resonance amplification factor = ratio  $\frac{A_d}{A_g}$   
 =  $A_v$  at resonance .
- $A_v$  = vibration amplification factor = ratio of amplitude of vibration to exciting amplitude  $A_g$  .
- $A_{re}$  =  $A_r$  under uniform stress distribution (tension-compression) at an excited stress equal to the fatigue strength  $S_e$  .
- $A_{re}^i$  =  $A_{re}$  for a part having non-uniform stress distribution and a maximum excited stress equal to the fatigue strength .
- CSSL** = cyclic stress sensitivity limit = maximum stress at which damping is not sensitive to sustained cyclic stress. (Psi).
- D** = specific damping energy of a material or that associated with a specific stress. Only if specimen is uniformly loaded is  $D = D_a$  , otherwise the average damping determined from  $D_o/V$  is smaller than the specific damping energy, in some cases considerably smaller. In-lb per cu-in per cycle.
- $D_a$  = average damping energy for a specimen or part =  $D_o/V$  .  
 In-lb per cu-in per cycle.
- $D_e$  = specific damping energy at the fatigue strength  $S_e$  . (In-lb per cu-in per cycle).
- $D_L$  = damping at cyclic stress sensitivity limit  $S_L$  . (In-lb per cu-in per cycle).
- $D_o$  = total internal damping energy dissipated by part. (In-lbs per cycle).
- $D_x$  = total external damping energy dissipated by a part. (In-lbs per cycle).
- E** = modulus of elasticity, psi. In this paper no distinction is made between static and dynamic modulus or average and specific values. (Psi).
- $F_g$  = alternating force which excites a vibrating system. (Lbs).
- J, J', etc.** = damping constant in exponential equations.
- $K_c$  = cross-sectional shape factor

- $K_s$  = longitudinal stress-distribution factor.
- $K_v$  = volume-stress factor of the part, which depends on its volume-stress function and a material damping characteristics. To be used when  $K_s$  and  $K_c$  can not be separated, otherwise  $K_v = K_s \cdot K_c$ .
- $n$  = damping exponent as defined in equation  $D = J S^n$ .
- $S$  = unit normal stress at any point in specimen. (Psi).
- $S_c$  = maximum or crest stress imposed during a stress cycle. (Psi).
- $S_d$  = excited stress excited at resonance by exciting force  $F_g$ . (Psi).
- $S_e$  = fatigue strength of a material at  $2 \times 10^7$  cycles. (Psi).
- $S_g$  = resonance exciting stress. Maximum stress which would exist in a part if exciting force  $F_g$  were applied at a frequency considerably below resonance where the vibration amplification  $A_v$  is equal to 1. For a part in which the external force is applied to a concentrated mass this would be equal to the maximum static stress caused by the external force. For a part having a distribution of mass which produces significant inertia loading during the vibration, the shape of the elastic curve of the part must be considered. (Psi).
- $S_{ge}$  = resonant strength constant of the material = exciting stress  $S_g$  which is required to produce excited stress  $S_d$  equal to fatigue limit  $S_e$  under uniform stress. (Psi).
- $S'_{ge}$  = resonant strength of a part = maximum exciting stress  $S_g$  which a part can withstand without exceeding the fatigue strength  $S_e$ .  $S'_{ge} = S_{ge}/K_v$ . (Psi).
- $S_L$  = stress at the cyclic stress sensitivity limit CSSL. (Psi)
- $T$  = ratio of specific damping energy  $D$  to average value  $D_a$ .
- $V$  = volume of test specimen or part having a stress less than  $S$ . (Cu-in).
- $V_o$  = total effective volume of specimen or part contributing to dissipation of damping energy  $D_o$  or elastic energy  $W_o$ . (Cu-in).
- $W_o$  = total elastic energy in member at maximum stress. (In-lb).

TABLE I SOURCE, CHEMICAL COMPOSITION, PRODUCTION, HEAT TREATM

Name of Material	Source	Chemical Composition Per Cent	Pi
Sandvik Steel (quenched-tempered)	Sandvikens Jernverks Aktiebolag Sandviken, Sweden	Cr 1.02, Si 0.22, Ni 0.01 C 0.98, S 0.014, Mn 0.26, P 0.028, Mo 0.24, Cu 0.02, Fe (bal)	Acid open stock. Hea Quenched
Sandvik Steel (normalized)	Sandvikens Jernverks Aktiebolag Sandviken, Sweden	Cr 1.02, Si 0.22, Ni 0.01, C 0.98, S 0.014, Mn 0.26, P 0.028, Mo 0.24, Cu 0.02, Fe (bal)	Acid open stock. No Cooled in s
Type 403 GE B50R 207 Alloy	Republic Steel * Cleveland, Ohio	C 0.110, Cr 12.20, Mn 0.51. N 0.06, Si 0.34, Mo 0.05, P 0.018, S 0.010, Al 0.03, Sn 0.0089	Electric fur Heated to 1 in oil. Ref Air cooled.
RC 130 B Titanium	Rem-Cru Titanium Inc. ** Midland, Pennsylvania	Material are melted in an inert gas atmosphere. Ingot for rolling. Hot rolled to required size on tool steel m resulting bars were annealed for one hour and shot blas  Specimens heat treated before final polish by heating t to go from 1250° to 1300° F). Slowly cooled in furnac heat treatment. .0012" removed on radius in final po	
RC-55 Titanium (cold-worked)	Rem-Cru Titanium Inc. Midland, Pennsylvania	C 0.1 (max) T (bal)	Ingot (15" dia.) working technic 1800°F temp. r Hot rolled-ann in 3 cold draw The intermediat ing to 1300° F
RC-55 Titanium (annealed)	Rem-Cru Titanium Inc. Midland, Pennsylvania	C 0.1 (max) T (bal)	Initially for Hot-rolled: 1450°-1550 at 1300° F.
N-155 Alloy	Universal-Cyclops Steel Corporation Bridleville, Pennsylvania	Cr 21.7, W 1.90, C 0.15, Ni 19.4, Mn 1.74, N 0.14, Co 19.0, Cb 0.76, Mo 2.76, Si 0.37, Fe 32.1 (bal)	15.5 in. ing Rolled to 1 quenched fr 1400° F for
Stellite 31 (as cast)	Haynes Stellite Division *** Union Carbide and Carbon Corporation Kokomo, Indiana	C 0.45, S 0.016, Fe 1.39, Mn 0.42, Cr 24.8, Si 0.93, Ni 10.4, P .01, W 7.26, Co (bal)	Cast in spec on diameter
SAE 1020 Steel	Crucible Steel Company Syracuse, New York	Mn 0.3-0.6, C 0.15-0.25, S 0.055 (max), P 0.45 (max), Fe (bal)	Electric mel of 1-5/8" d for uniformi
24S-T4 Aluminum	Aluminum Corporation of America, New Kensington, Pennsylvania	Cu 4.20, Si 0.14, Mg 1.46, Zn 0.07, Mn 0.63, Cr 0.02, Fe 0.30, Ti 0.02, Al (bal)	Rolled bars at 915° F.
J-1 Magnesium	Dow Chemical Company Midland, Michigan	Al 5.8-7.2, Cu 0.05 (max), Zn 0.4-1.5, Fe 0.005 (max), Si 0.3 (max), Mg (bal), Mn 0.15 (min)	Extruded bar condition.
Gray Iron	Straight Line Foundry and Machine Company Syracuse, New York	C 3.65, S 0.132, Si 2.46, Mn 0.73, P 0.265, Fe 92.75 (bal)	1-1/4" x 21
Glass Laminate Plastic	Cincinnati Testing and ** Research Laboratory Cincinnati, Ohio	CTL-91-LD Resin 181-114 Fiberglass	Resin impreg at approxime

COMPOSITION, PRODUCTION, HEAT TREATMENT, AND SPECIMEN SIZE OF TEST MATERIALS

2

Chemical Composition Per Cent	Production, Heat Treatment, Etc.	Specimen Diameter
.02, Si 0.22, Ni 0.01 .98, S 0.014, Mn 0.26, .028, Mo 0.24, Cu 0.02, al)	Acid open hearth steel hot-rolled to 1 in. hex. bar stock. Heated to 1515° F (15 minutes at heat). Quenched in oil. Drawn at 1095° F for one hour.	D = 0.375"
.02, Si 0.22, Ni 0.01, .98, S 0.014, Mn 0.26, .028, Mo 0.24, Cu 0.02, al)	Acid open hearth steel hot-rolled to 1 in. hex. bar stock. Normalized by resistance heating to 1905° F. Cooled in still air.	D = 0.375"
.110, Cr 12.20, Mn 0.51. .06, Si 0.34, Mo 0.05, .018, S 0.010, Al 0.03, .0089	Electric furnace alloy hot-rolled to 1 in. round. Heated to 1750° F (15 minutes at heat), quenched in oil. Reheated to 1050° F for 1-1/2 hours. Air cooled.	D = 0.250"
Material are melted in an inert gas atmosphere. Ingot was hammer forged to suitable billet size following. Hot rolled to required size on tool steel mill. Rolling temperature 1500° F. The ingot bars were annealed for one hour and shot blasted. Specimens heat treated before final polish by heating to 1300° F in 16 hours (2 hours required from 1250° to 1300° F). Slowly cooled in furnace. No special atmosphere used in this treatment. .0012" removed on radius in final polish.		D = 0.206"
.1 (max) al)	Ingot (15" dia.) was forged and hot rolled 1" dia. per best hot working technique. The material was hot worked in the 1500-1800° F temp. range and annealed at 1300° F, and air cooled. Hot rolled-annealed 1" dia. bar was cold drawn to 7/8" dia. in 3 cold drawn passes of approximately 6% reduction each. The intermediate and final heat treatment consisted of heating to 1300° F followed by air cooling.	D = 250"
.1 (max) l)	Initially forged in temperature range 1700°-1800° F. Hot-rolled to finish size 7/8" in temperature range 1450°-1550° F and finally annealed for one hour at 1300° F.	D = 0.250"
.7, W 1.90, C 0.15, .4, Mn 1.74, N 0.14, .0, Cb 0.76, Mo 2.76, 37, Fe 32.1 (bal)	15.5 in. ingot hammer clogged to 2 in. square. Rolled to 1 in. rounds at 2050°-1830° F. Water quenched from 2200° F. Aging treatment - 1400° F for 16 hours, air cooled.	D = 0.206"
.45, S 0.016, Fe 1.39, .42, Cr 24.8, Si 0.93, .4, P .01, W 7.26, al)	Cast in specimen form. .0050" - .010" removed on diameter in finish polishing.	D = 0.250"
.3-0.6, C 0.15-0.25, .55 (max), P 0.45 (max), al)	Electric melted steel hot-rolled to round bar stock of 1-5/8" diameter. Steel especially controlled for uniformity and cleanliness.	D = 0.250"
.20, Si 0.14, Mg 1.46, .07, Mn 0.63, Cr 0.02, 30, Ti 0.02, Al (bal)	Rolled bars 1-1/8" diameter. Solution heat treated at 915° F.	D = 0.585"
8-7.2, Cu 0.05 (max), .4-1.5, Fe 0.005 (max), 3 (max), Mg (bal), .15 (min)	Extruded bars 1-5/8" diameter, used in this condition.	D = 0.585"
.05, S 0.132, Si 2.46, .73, P 0.265, Fe 92.75 (bal)	1-1/4" x 20" regular arbitration bars, as cast.	D = 0.585"
1-LD Resin 14 Fiberglass	Resin impregnated into fiberglass fabric and pressed at approximately 15 psi into panel 1-1/4" thick.	D = 0.275"
2		Typical Specimen Shape ..... N"R

N-155 Alloy	Universal-Cyclops Steel Corporation Bridleville, Pennsylvania	Cr 21.7, W 1.90, C 0.15, Ni 19.4, Mn 1.74, N 0.14, Co 19.0, Cb 0.76, Mo 2.76, Si 0.37, Fe 32.1 (bal)	15.5 in. ingot hammer cc Rolled to 1 in. rounds at quenched from 2200° F. 1400° F for 16 hours, air
Stellite 31 (as cast)	Haynes Stellite Division *** Union Carbide and Carbon Corporation Kokomo, Indiana	C 0.45, S 0.016, Fe 1.39, Mn 0.42, Cr 24.8, Si 0.93, Ni 10.4, P .01, W 7.26, Co (bal)	Cast in specimen form . on diameter in finish poli
SAE 1020 Steel	Crucible Steel Company Syracuse, New York	Mn 0.3-0.6, C 0.15-0.25, S 0.055 (max), P 0.45 (max), Fe (bal)	Electric melted steel hot- of 1-5/8" diameter. Stee for uniformity and cleanli
24S-T4 Aluminum	Aluminum Corporation of America, New Kensington, Pennsylvania	Cu 4.20, Si 0.14, Mg 1.46, Zn 0.07, Mn 0.63, Cr 0.02, Fe 0.30, Ti 0.02, Al (bal)	Rolled bars 1-1/8" diame at 915° F.
J-1 Magnesium	Dow Chemical Company Midland, Michigan	Al 5.8-7.2, Cu 0.05 (max), Zn 0.4-1.5, Fe 0.005 (max), Si 0.3 (max), Mg (bal), Mn 0.15 (min)	Extruded bars 1-5/8" dian condition.
Gray Iron	Straight Line Foundry and Machine Company Syracuse, New York	C 3.65, S 0.132, Si 2.46, Mn 0.73, P 0.265, Fe 92.75 (bal)	1-1/4" x 20" regular arb
Glass Laminate Plastic	Cincinnati Testing and ** Research Laboratory Cincinnati, Ohio	CTL-91-LD Resin 181-114 Fiberglass	Resin impregnated into fil at approximately 15 psi ii

\*Procured through General Electric Company, Metallurgical Development Unit,  
Plant Laboratory, Building 200, Lockland 15, Ohio.

\*\*Procured through Wright Air Development Center, Wright-Patterson Air Force  
Base, Ohio, Attention: WCRTL-5, Materials Laboratory.

\*\*\*Procured through Westinghouse Electric Corporation, Aviation Gas Turbine  
Division, Philadelphia 13, Pennsylvania.

3

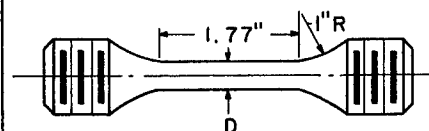
<p>C / 1.90, C 0.15, Mn 1.74, N 0.14, P 0.76, Mo 2.76, S 32.1 (bal)</p>	<p>15.5 in. ingot hammer cogged to 2 in. square. Rolled to 1 in. rounds at 2050°-1830° F. Water quenched from 2200° F. Aging treatment - 1400° F for 16 hours, air cooled.</p>	<p>D = 0.206"</p>
<p>C 0.016, Fe 1.39, Cr 24.8, Si 0.93, S .01, W 7.26,</p>	<p>Cast in specimen form. .0050" - .010" removed on diameter in finish polishing.</p>	<p>D = 0.250"</p>
<p>C C 0.15-0.25, P 0.45 (max),</p>	<p>Electric melted steel hot-rolled to round bar stock of 1-5/8" diameter. Steel especially controlled for uniformity and cleanliness.</p>	<p>D = 0.250"</p>
<p>Mg Mg 1.46, Mn 0.63, Cr 0.02, Si 0.02, Al (bal)</p>	<p>Rolled bars 1-1/8" diameter. Solution heat treated at 915° F.</p>	<p>D = 0.585"</p>
<p>Cu Cu 0.05 (max), Fe 0.005 (max), Mg (bal), Zn</p>	<p>Extruded bars 1-5/8" diameter, used in this condition.</p>	<p>D = 0.585"</p>
<p>Si Si 2.46, S 0.265, Fe 92.75 (bal)</p>	<p>1-1/4" x 20" regular arbitration bars, as cast.</p>	<p>D = 0.585"</p>
<p>Resin Resin  fiberglass</p>	<p>Resin impregnated into fiberglass fabric and pressed at approximately 15 psi into panel 1-1/4" thick.</p>	<p>D = 0.275"</p>

Unit,

Force

ine

Typical Specimen Shape



Slightly Tapered Test Section

4

4

TABLE II DAMPING, ELASTICITY,

Type of Material	Material (and Test Temp. If Above Room Temp.)	CSSL $S_L$ KSI	Fatigue Strength $S_e$ KSI	Ratio $S_L/S_e$	Mod. of Elas. $E$ psi $\times 10^{-6}$	Yield Str. 0.2% Offset KSI	Tensile Strength KSI
Super Alloys	Type 403	70.	65.	1.07	30.5	111.	129.
	N-155	33.	53.	0.62	30.0	60.5	119.
	N-155 1350° F	26.	40.	0.65	22.3		
	N-155 1500° F	25.	29.	0.86	21.3		
	Stellite 31 AC				32.9	65.1	92.6
	Stellite 31 AC 1200° F	24.	38.	0.63	28.2		
	Stellite 31 AC 1350° F	35.	38.	0.92	26.4		
	Stellite 31 AC 1500° F	33.	32.	1.03	25.4		
Titanium	RC130B	95.	86.	1.10	16.9	139.	152.
	RC130B 600° F	50.	62.	0.81	14.5		
	RC55 CW	15.	45.	0.33	14.6	81.6	87.
	RC55 CW 600° F	20.	22.	0.89	11.5		
	RC55 A	24.	41.	0.59	13.8	57.05	75.7
	RC55 A 600° F	10.5	20.5	0.48	10.6		
Other Ferrous Materials	Sandvik (Q & T)	100.	92.	1.09	29.2	177.	204.
	Sandvik (N)	55.	76.	0.72	29.2	116.5	186.
	SAE 1020 Steel	30.	35.5	0.85	29.4	46.6	71.3
	Gray Iron	6.5	9.5	0.69	19.4		20.3
Other Non-Ferrous Metals	24S-T4 Aluminum	24.	27.	0.88	10.6	48.6	72.8
	J-1 Magnesium	8.	17.	0.47	6.5	33.5	46.
Non-Metals	Glass Laminate	>18.	11.	>1.6	3.4		40.

\*Up to 12 KSI beyond 12 KSI  $n = 1.5$  at 20 KSI, 1.05 at 30 KSI, 0.63 at 40, 50, and 60 KSI

\*\*This value based on damping at maximum number of cycles of stress history.

DAMPING, ELASTICITY, FATIGUE, AND STATIC PROPERTIES OF VARIOUS STRUCTURAL MATERIALS

Yield Str. (.2% Offset KSI)	Tensile Strength KSI	Elong. in 2 in. %	Reduction of Area %	Hardness	Damping Properties						
					Up To CSSL			D at	D at S <sub>e</sub> After		
					J · 10 <sup>12</sup>	n	D <sub>L</sub>	60% S <sub>e</sub>	10 <sup>1.3</sup> Cycles	10 <sup>6</sup> Cycles	
111. 60.5	129. 119.	21. 43.7	65. 46.	R <sub>c</sub> 25	.25* 2.0 .13 0.19	2.9* 2.5 3.0 3.0	1.85 0.4 2.3 3.	0.78 0.4 1.8 1.0	1.4 45. 140. 10.	1.4 25. 14. 11.	
65.1	92.6	5.	5.5	R <sub>c</sub> 27.3	0.14 774. 4,040.	2.9 2.1 2.0	0.7 2.7 4.4	0.6 1.1 1.6	8. 12. 4.2	0.9 3. 4.2	
139. 81.6	152. 87.		34.2 32.	R <sub>c</sub> 35.8	274. 520. 28.8 176.	2.0 2.0 2.2 2.2	2.1 1.3 0.046 0.52	0.65 0.72 1.15 0.22	1.75 1.9 6. 3.3	1.75 5. 20. 1.8	
57.05	75.7	24.5	25.	R <sub>c</sub> 15.9	278. 590.	2.0 2.0	0.16 0.065	0.17 0.5	11. 38.	150. 10.	
177. 116.5 46.6	204. 186. 71.3 20.3		21. 11. 60.5		8.9 0.61 500. 494.	2.3 2.6 2.0 2.4	2.8 1.3 0.45 0.7	0.8 0.8 0.23 0.5	2.3 12. 0.7 2.	2.3 70. 20. 1.2	
48.6 33.5	72.8 46.	21.4 14.5			780. 1,560.	2.0 2.0	0.45 0.1	0.2 0.13	1. 1.1	0.6 0.5	
	40.				4.2	2.9		0.5	2.	2.	

), and 60 KSI

Resonant Strength Constant  $S_{ge} = \frac{E D_e}{S_e}$

STRUCTURAL MATERIALS

Damping Properties						Exciting Stress $S_g^{**}$ in PSI to Produce Excited Stress $S_d$ Equal to			
SL	D at	D at $S_e$ After		D at 120% $S_e$		60% $S_e$	$S_e$	120% $S_e$	
	$D_L$	60% $S_e$	$10^{1.3}$ Cycles	$10^6$ Cycles	$10^{1.3}$ Cycles	Max. No. of Cycles			
	1.85	0.78	1.4	1.4	5.	10.	194.	210.	1,245.
	0.4	0.4	45.	25.	180.	220.	120.	4,550.	33,000.
	2.3	1.8	140.	14.	700.	30.	530.	2,480.	4,430.
	3.	1.0	10.	11.	50.	60.	390.	2,570.	11,700.
	0.7	0.6	8.	0.9	50.	20.	230.	210.	3,940.
	2.7	1.1	12.	3.	200.	13.	400.	660.	2,400.
	4.4	1.6	4.2	4.2	23.	11.	670.	1,050.	2,300.
	2.1	0.65	1.75	1.75	2.7	3.5	68.	109.	183.
	1.3	0.72	1.9	5.	4.4	25.	89.	372.	1,550.
	0.046	1.15	6.	20.	13.	100.	198.	2,070.	8,460.
	0.52	0.22	3.3	1.8	9.8	16.	61.	300.	2,210.
	0.16	0.17	11.	150.	50.	75.	30.	16,100.	6,700.
	0.065	0.5	38.	10.	65.	40.	140.	1,650.	5,490.
	2.8	0.8	2.3	2.3	4.5	30.	130	230.	250.
	1.3	0.8	12.	70.	100.	220.	160.	8,550.	22,400.
	0.45	0.23	0.7	20.	5.	100.	100.	5,270.	21,900.
	0.7	0.5	2.	1.2	3.3	2.3	540.	780.	1,240.
	0.45	0.2	1.	0.6	0.95	2.2	42.	75.	230.
	0.1	0.13	1.1	0.5	3.5	1.	25.	60.	100.
		0.5	2.	2.	3.3	3.3	88.	212.	290.

Instant

$$S_{ge} = \frac{E D_e}{S_e}$$

TABLE III  
EFFECT OF HEAT TREATMENT ON PROPERTIES OF AN ALLOY STEEL PART  
AT RESONANCE, BOTH AS A MATERIAL (OR UNIFORM-STRESS PART) AND  
A PART HAVING HIGH  $K_v$ .

Property	SANDVIK STEEL		
	Quenched & Tempered	Normalized	
$S_e$ , psi	92,000	76,000	Material Properties
$E$ , psi	$29.2 \times 10^6$	$29.2 \times 10^6$	
$D_e$ at max N	2.3	70	
$A_{re}$ , unitless	400	8.9	
$S_{ge}$ , psi	230	8,550	
$K_v$ , unitless	1.45	22.4	Part Properties as a turbine blade
$A'_{re} = A_{re} K_v$	580	200	
$S'_{ge}$ , psi	160	380	

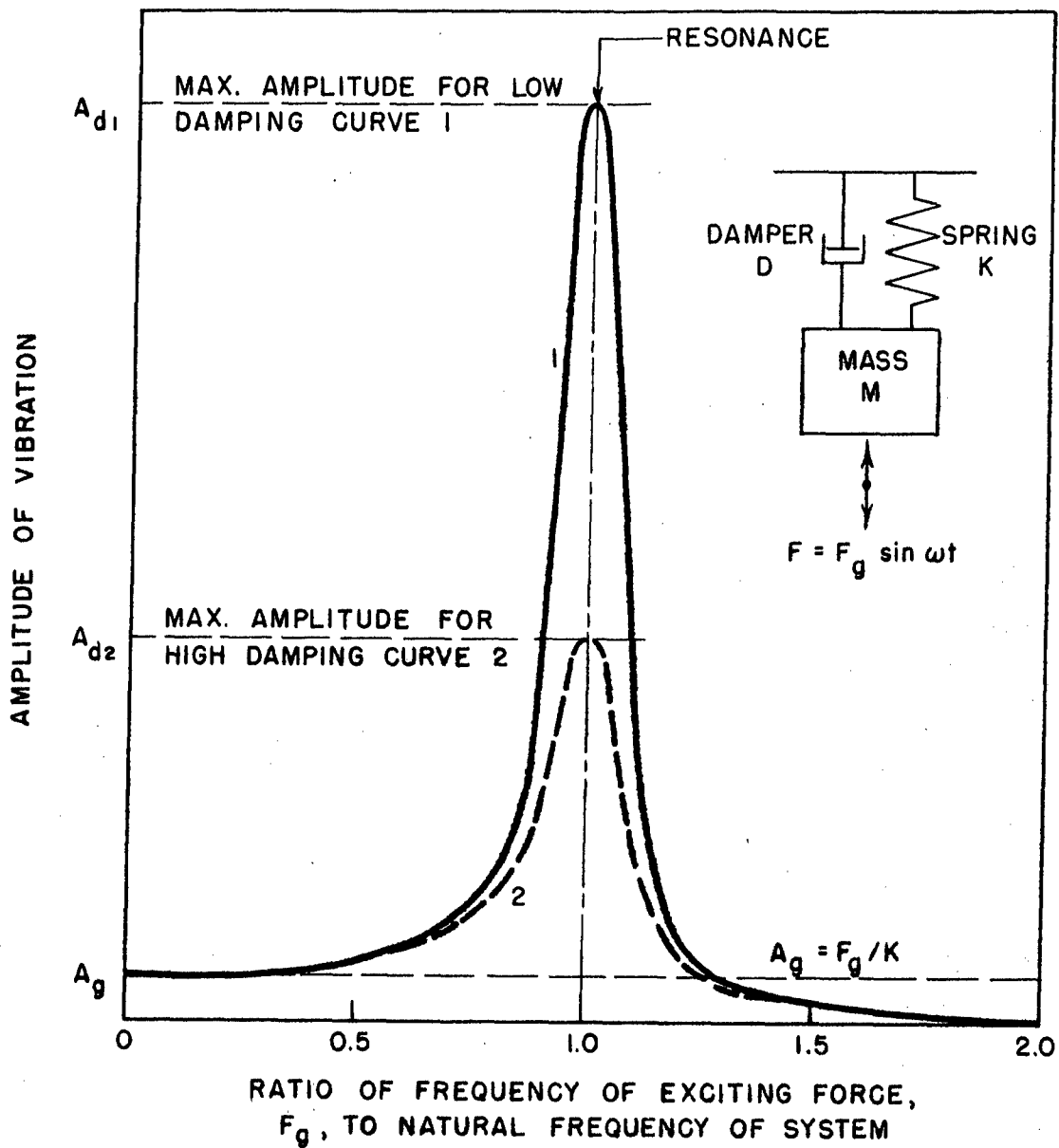


FIG. I. EFFECT OF DAMPING ON AMPLITUDE OF NEAR-RESONANCE VIBRATION.

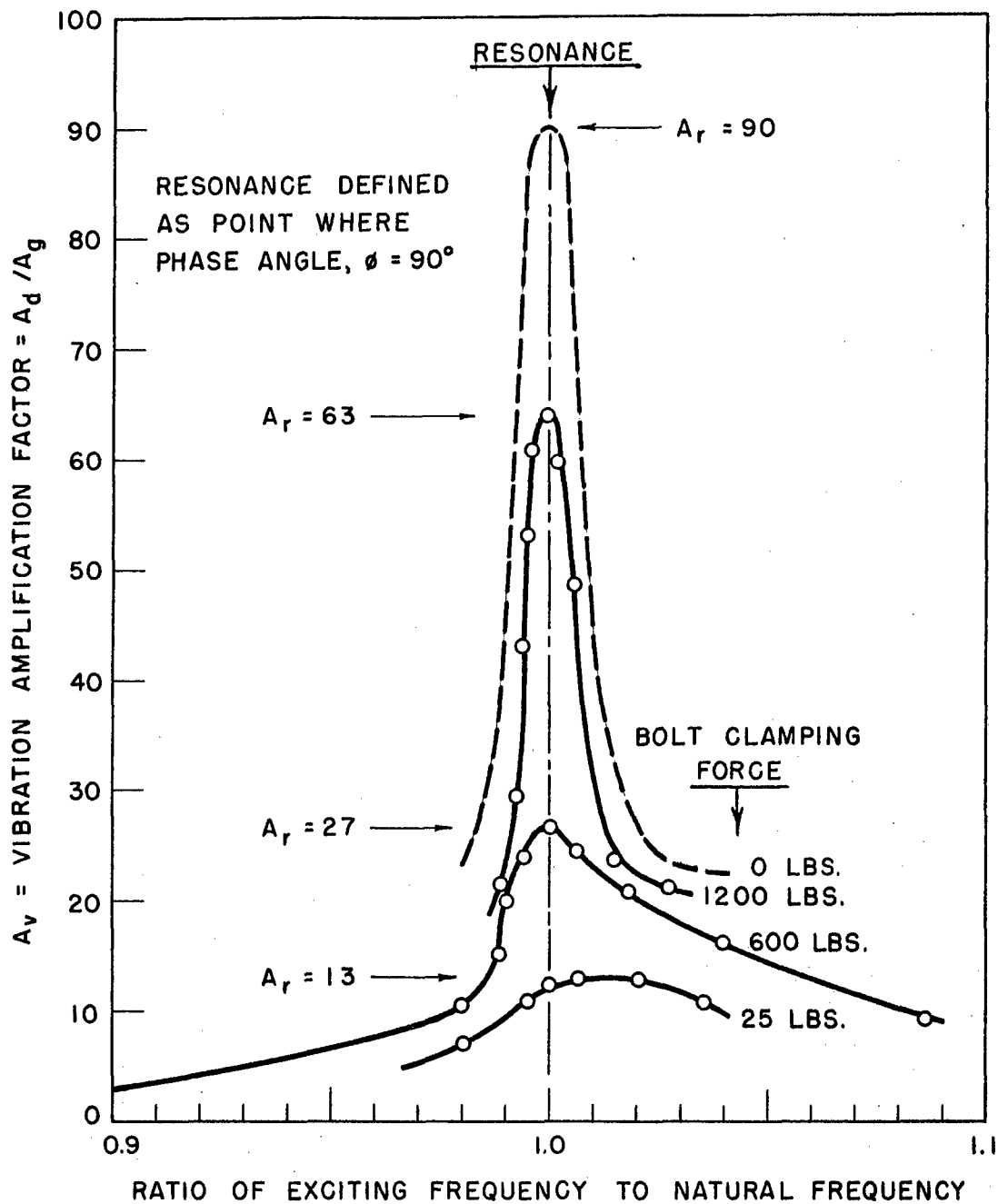
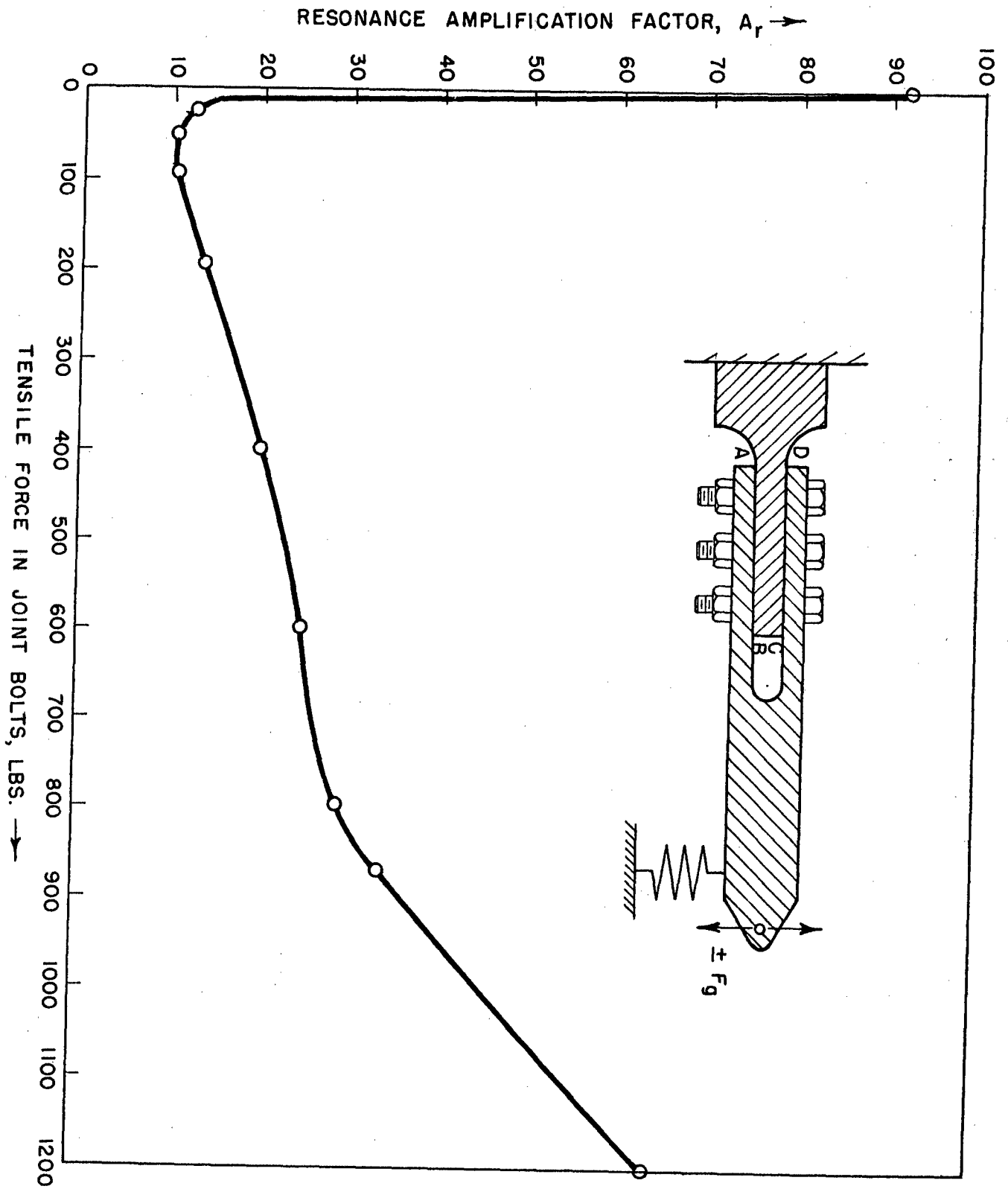


FIG. 2. RESONANCE CURVES FOR A BOLTED CONNECTION, INDICATING EFFECT OF BOLT CLAMPING FORCE.

FIG. 3. EFFECT OF JOINT BOLT PRESSURE ON RESONANCE AMPLIFICATION FACTOR.



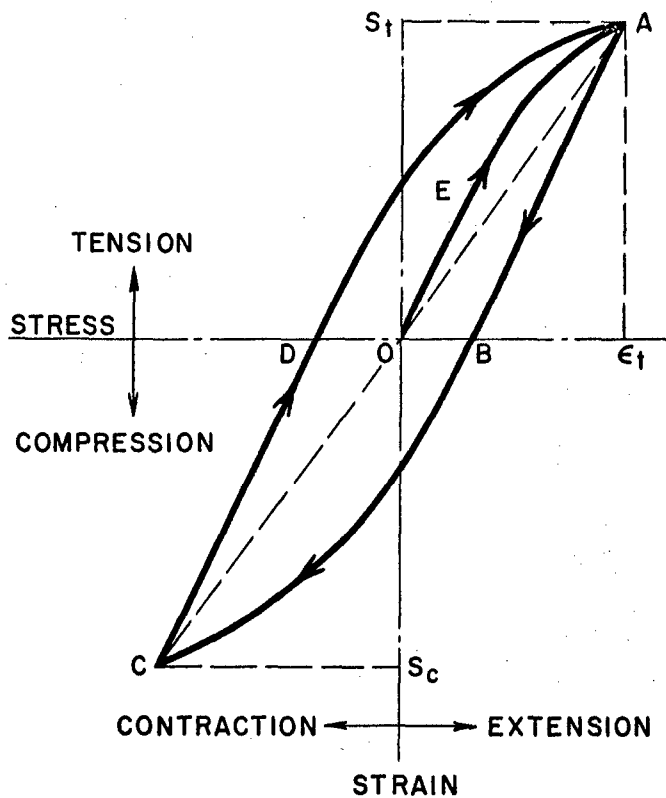


FIG. 4. TYPICAL STRESS-STRAIN HYSTERESIS LOOP FOR MATERIAL UNDER REVERSED AXIAL STRESS.

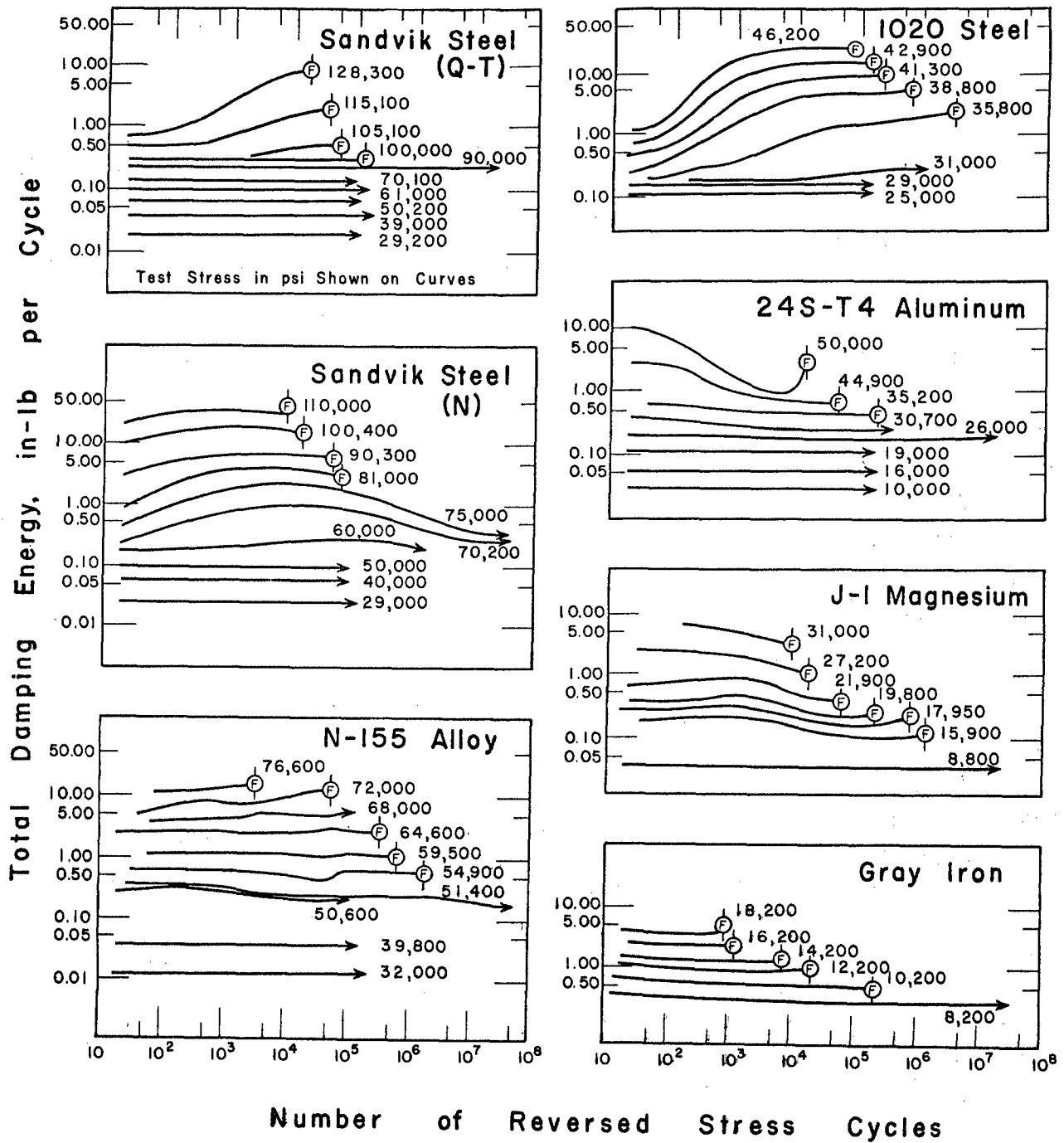


Fig. 5 - Comparison of the Effect of Sustained Cyclic Stress of Several Magnitudes on the Total Damping Energy of Various Materials.

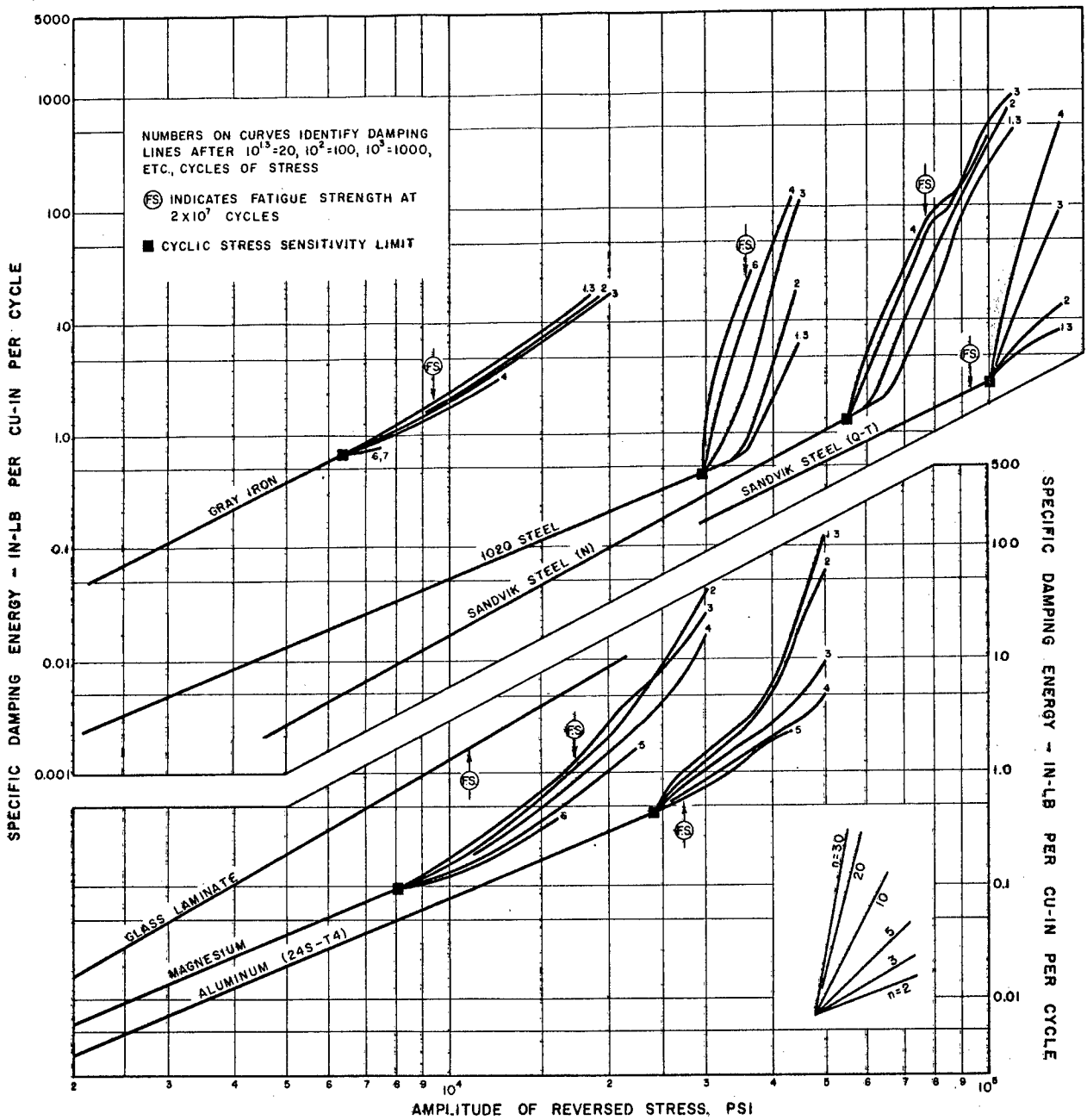


FIG. 6 SPECIFIC DAMPING ENERGY AS A FUNCTION OF AMPLITUDE OF REVERSED STRESS FOR GLASS LAMINATE, MAGNESIUM, ALUMINUM (24S-T4), GRAY IRON, 1020 STEEL, SANDVIK STEEL (N), AND SANDVIK STEEL (Q-T).

DAMPING ENERGY, D, IN-LB PER CU-IN PER CYCLE

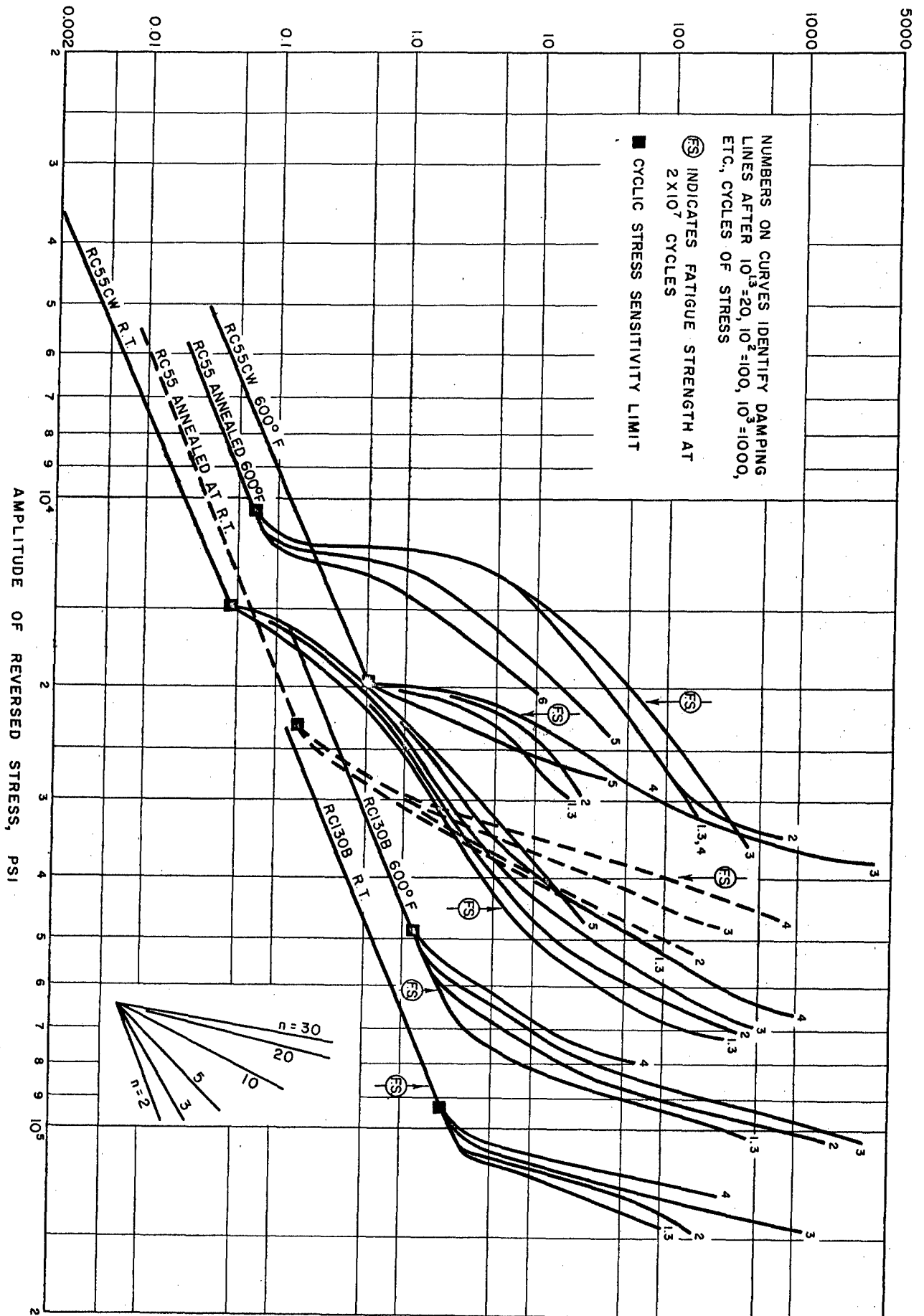


FIG. 7 SPECIFIC DAMPING ENERGY AS A FUNCTION OF AMPLITUDE OF REVERSED STRESS FOR TITANIUM (RC55 ANNEALED, RC55 COLD-WORKED, AND RC130B) AT 600° F AND ROOM TEMPERATURE.

FIG. 8 SPECIFIC DAMPING ENERGY AS A FUNCTION OF AMPLITUDE OF REVERSED STRESS FOR TYPE 403 AT ROOM TEMPERATURE, N-155 AT ROOM TEMPERATURE, 1350°, AND 1500° F, AND STELLITE 31 AS CAST AT 1200°, 1350° AND 1500° F.

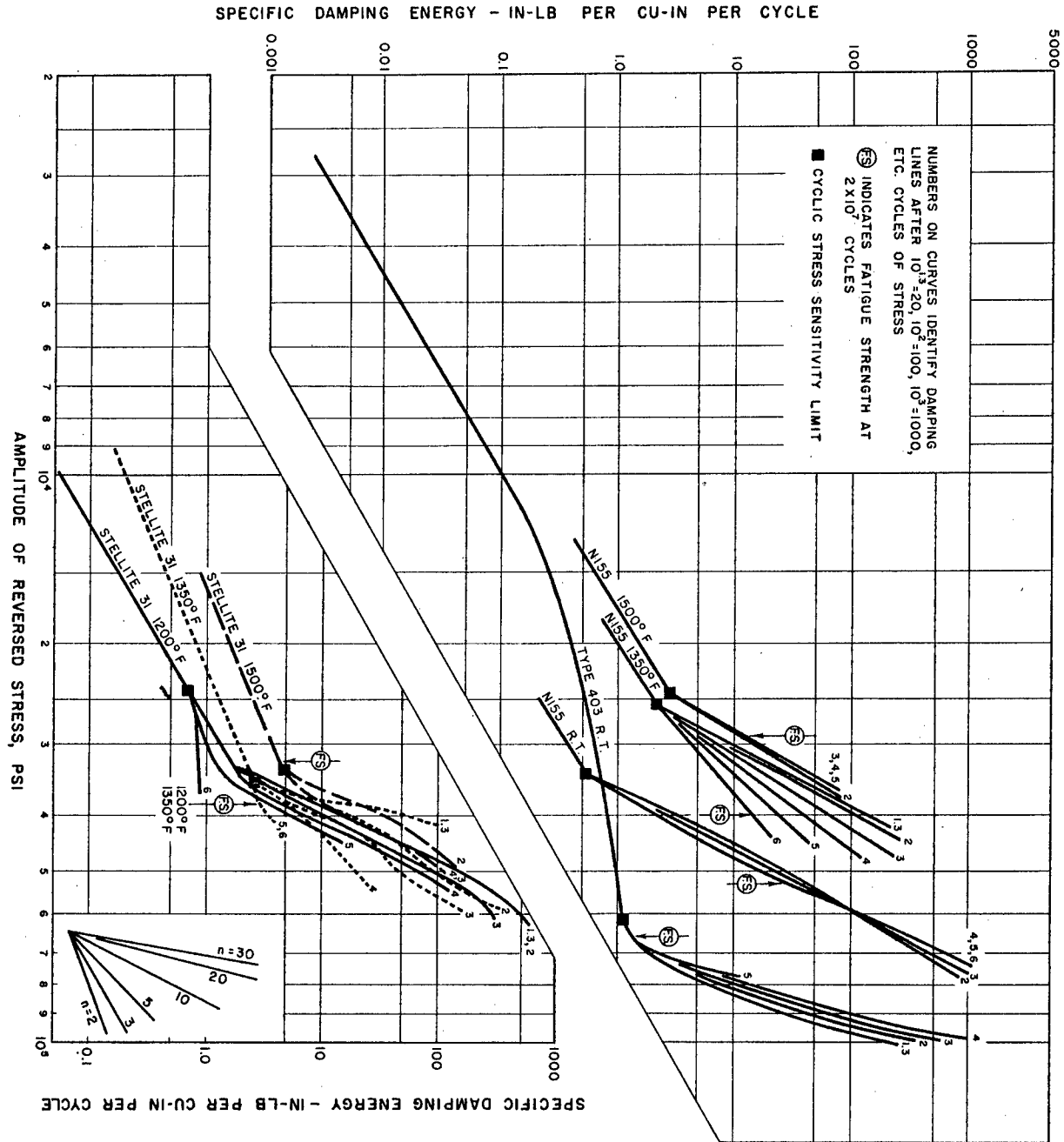


FIG. 9 DEPENDENCE OF SPECIFIC DAMPING ENERGY OF VARIOUS STRUCTURAL MATERIALS UPON RATIO OF CYCLIC STRESS TO FATIGUE STRENGTH.

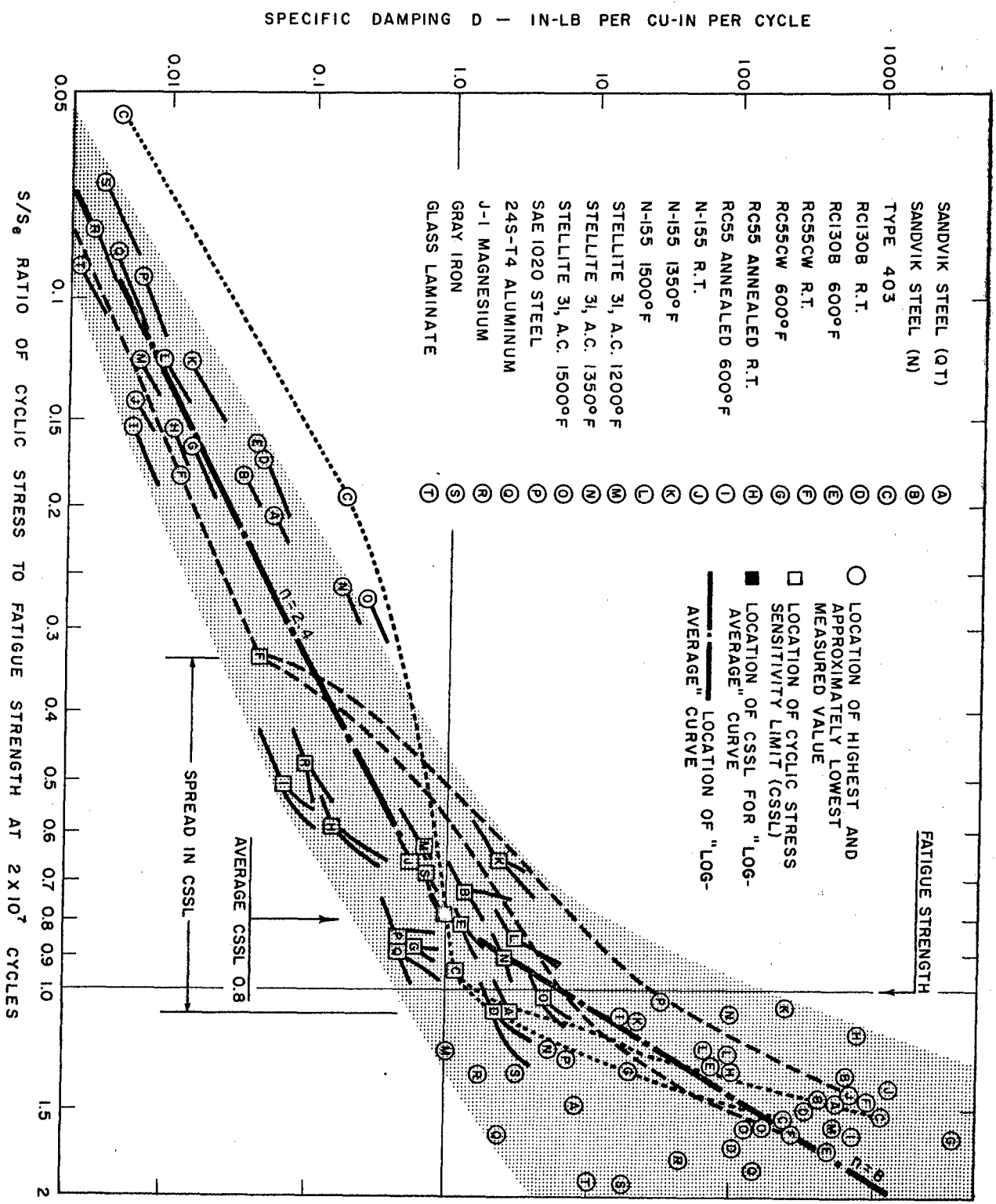
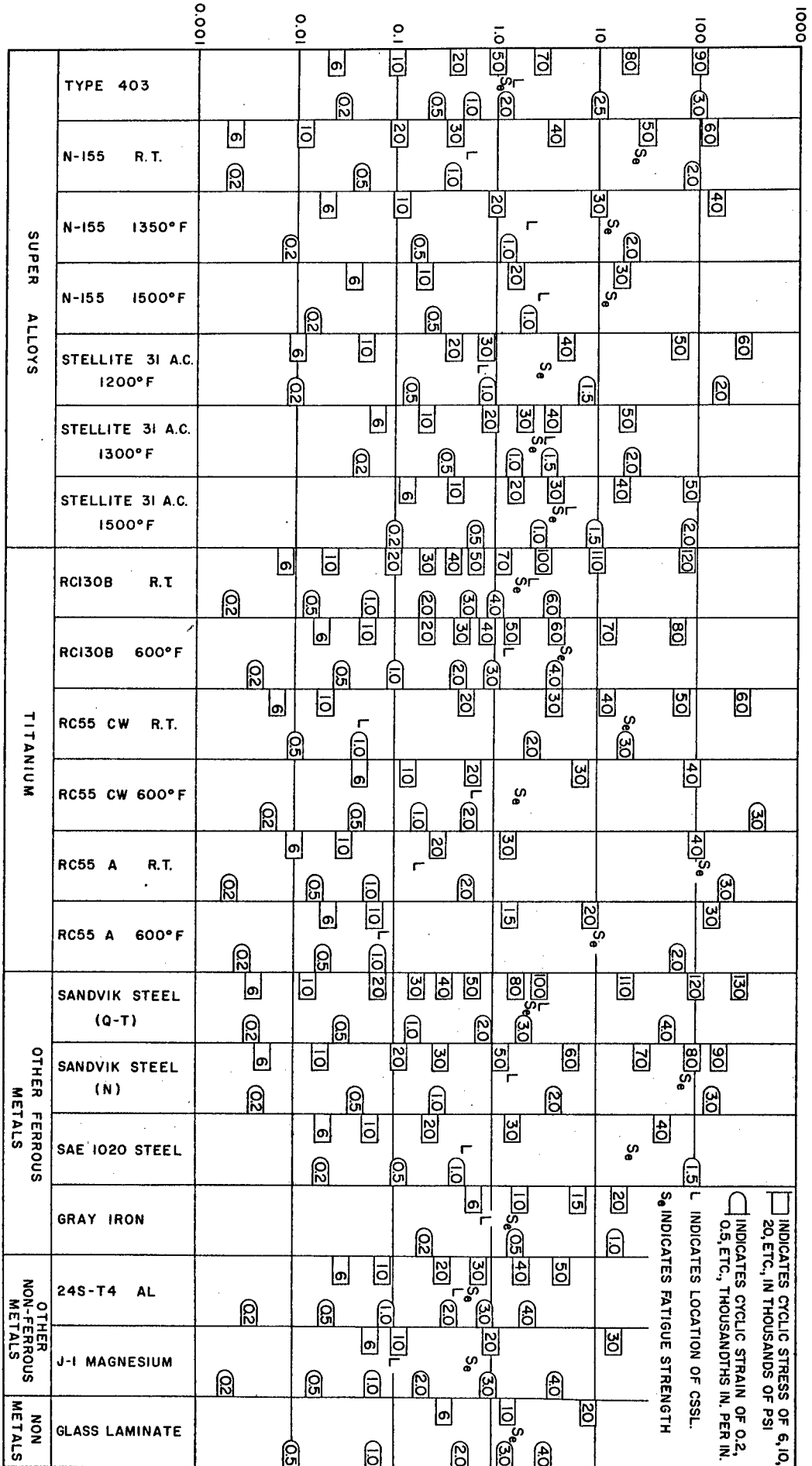


FIG. 10 DAMPING ENERGY OF VARIOUS STRUCTURAL MATERIALS AT STRESSES AND STRAINS IN THE ENGINEERING RANGE.



SPECIFIC DAMPING ENERGY, D, IN-LB PER CU-IN PER CYCLE

FIG. II SPECIFIC DAMPING ENERGY AT VARIOUS RATIOS OF CYCLIC STRESS TO FATIGUE STRENGTH FOR VARIOUS STRUCTURAL MATERIALS.

		0.01	0.1	1.0	10	100	1000
SUPER ALLOYS	TYPE 403						
	N-155 R.T.	-0.2	-0.4	-0.6	-0.8	-1.0	-1.2
	N-155 1350°F	-0.2	-0.4	-0.6	-0.8	-1.0	-1.2
	N-155 1500°F	-0.2	-0.4	-0.6	-0.8	-1.0	-1.2
	STELLITE 3I A.C. 1200°F	-0.2	-0.4	-0.6	-0.8	-1.0	-1.2
	STELLITE 3I A.C. 1350°F	-0.2	-0.4	-0.6	-0.8	-1.0	-1.2
	STELLITE 3I A.C. 1500°F	-0.2	-0.4	-0.6	-0.8	-1.0	-1.2
TITANIUM	RC130B R.T.	-0.2	-0.4	-0.6	-0.8	-1.0	-1.2
	RC130B 600°F	-0.2	-0.4	-0.6	-0.8	-1.0	-1.2
	RC55 CW R.T.	-0.2	-0.4	-0.6	-0.8	-1.0	-1.2
	RC55 CW 600°F	-0.2	-0.4	-0.6	-0.8	-1.0	-1.2
	RC55 A R.T.	-0.2	-0.4	-0.6	-0.8	-1.0	-1.2
	RC55 A 600°F	-0.2	-0.4	-0.6	-0.8	-1.0	-1.2
	OTHER FERROUS METALS	SANDVIK STEEL (Q-T)	-0.2	-0.4	-0.6	-0.8	-1.0
SANDVIK STEEL (N)		-0.2	-0.4	-0.6	-0.8	-1.0	-1.2
SAE 1020 STEEL		-0.2	-0.4	-0.6	-0.8	-1.0	-1.2
GRAY IRON		-0.2	-0.4	-0.6	-0.8	-1.0	-1.2
OTHER NON-FERROUS METALS		24S-T4 AL	-0.2	-0.4	-0.6	-0.8	-1.0
	J-1 MAGNESIUM	-0.2	-0.4	-0.6	-0.8	-1.0	-1.2
	GLASS LAMINATE	-0.2	-0.4	-0.6	-0.8	-1.0	-1.2

NUMBERS IN COLUMNS INDICATE WHERE RATIO  $S = \frac{\text{CYCLIC STRESS}}{S_e}$  FATIGUE STRENGTH EQUALS 0.2, 0.4, ETC.

"L" SHOWS LOCATION OF CSSL.

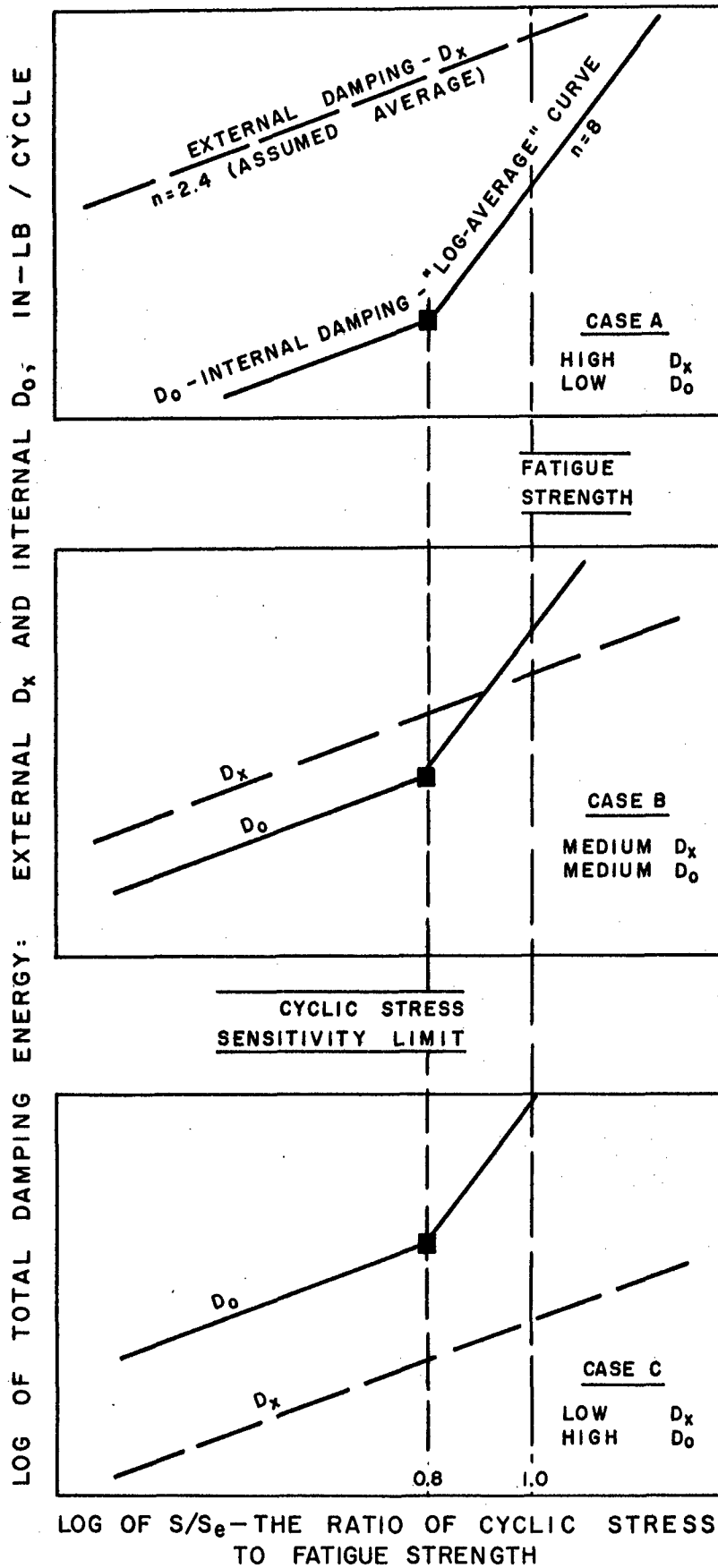


FIG. 12. SIMPLIFIED COMPARISON OF THE CONTRIBUTIONS OF EXTERNAL AND INTERNAL DAMPING TO A VIBRATING SYSTEM.

SPECIFIC DAMPING ENERGY D - IN-LB / CU-IN / CYCLE

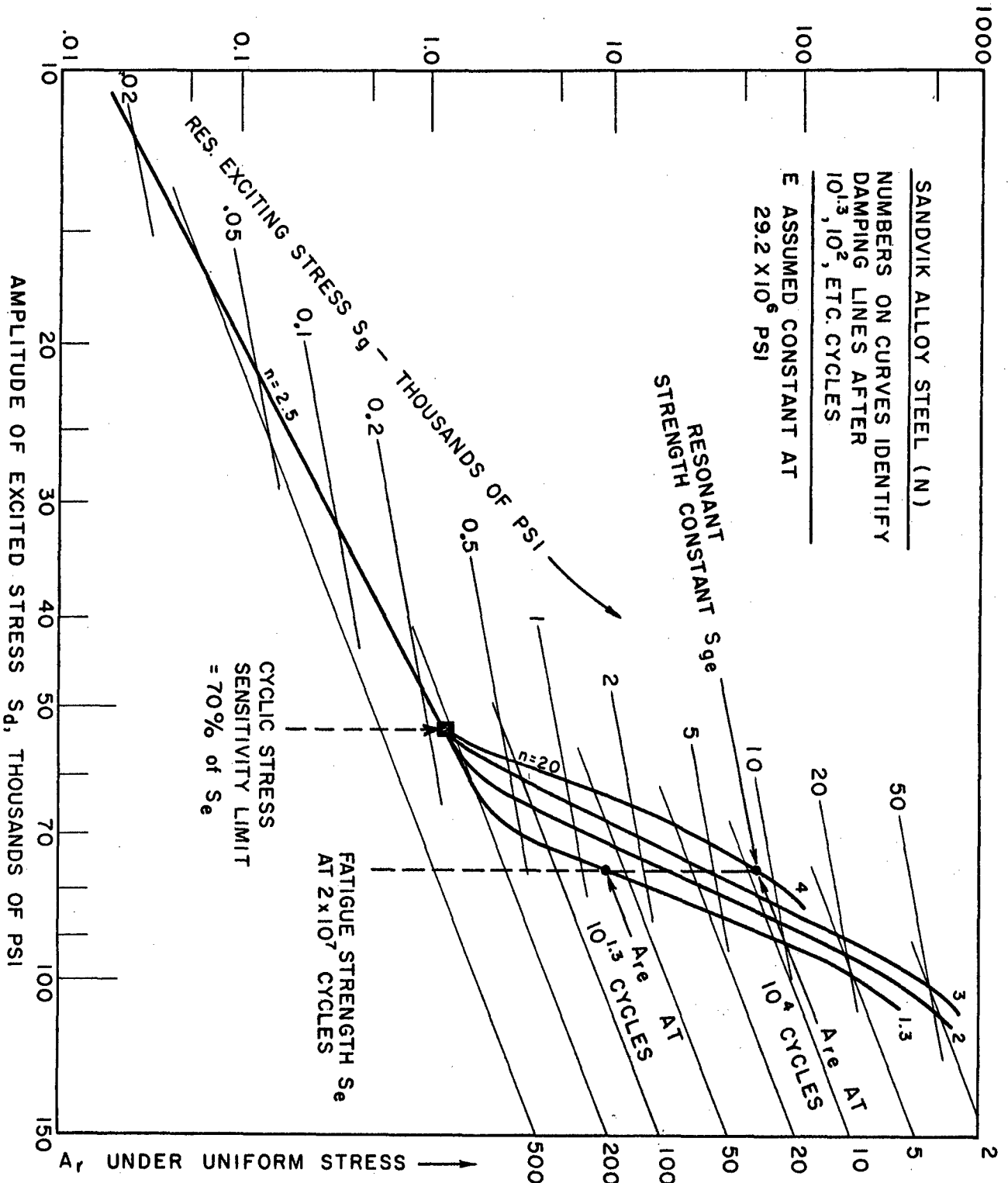
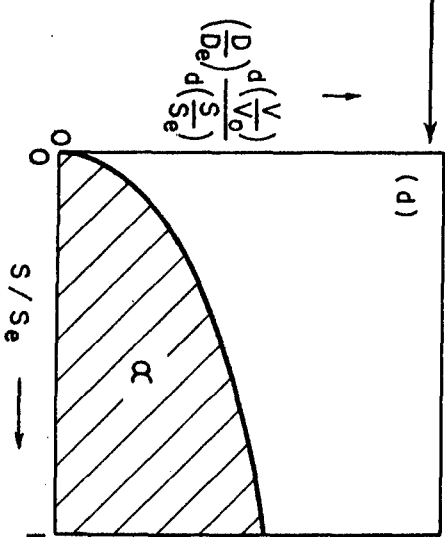
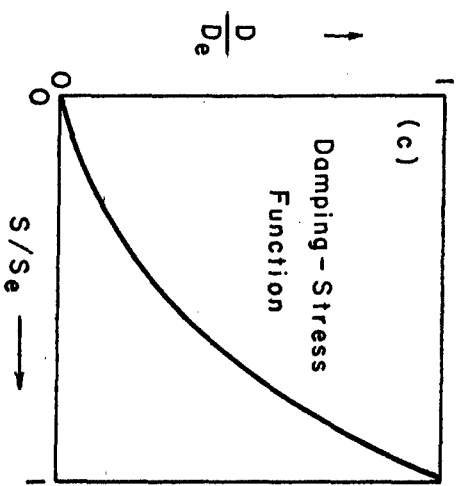
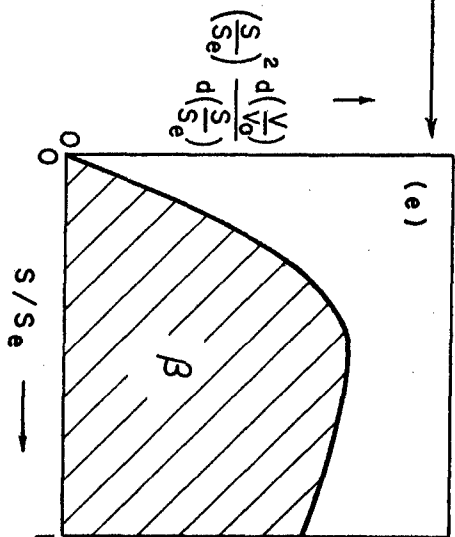
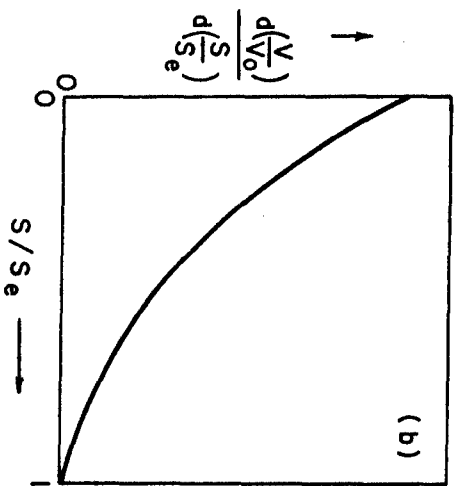
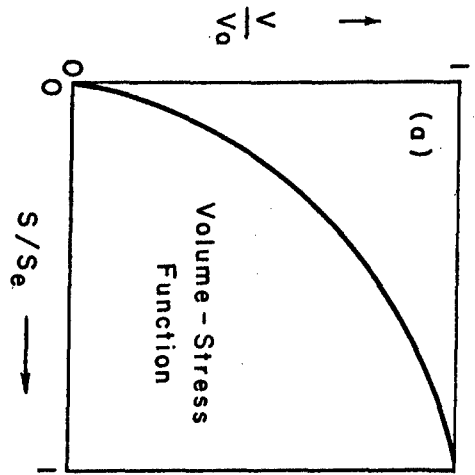


FIG. 13 DAMPING-STRESS CURVES FOR SANDVIK ALLOY STEEL, NORMALIZED SHOWING RESONANCE AMPLIFICATION FACTOR AND EXCITING STRESS GRIDS.

EXCITING STRESS  $S_0$  AND FATIGUE STRENGTH  $S_e$ , PSI

		10	50	100	500	1,000	5,000	10,000	50,000	100,000
SUPER ALLOYS	TYPE 403				-1.0 -0.6	-1.2			-Se	-Se
	N-155 R.T.	EXCITING STRESS $S_0$ (AT MAX. NUMBER OF CYCLES) TO PRODUCE AN EXCITED STRESS $S_e$ , EQUAL TO 60% $S_e$ LINES-0.6 100% $S_e$ LINES-1.0 120% $S_e$ LINES-1.2			-0.6		-1.0		-1.2	-Se
	N-155 1350° F				-0.6		-1.0		-1.2	-Se
	N-155 1500° F				-0.6		-1.0		-1.2	-Se
	STELLITE 3I A.C. 1200° F				-0.6		-1.0		-1.2	-Se
	STELLITE 3I A.C. 1350° F				-0.6		-1.0		-1.2	-Se
	STELLITE 3I A.C. 1500° F				-0.6		-1.0		-1.2	-Se
TITANIUM	RC130B R.T.		-0.6	-1.0	-1.2				-Se	-Se
	RC130B 600° F		-0.6	-1.0	-1.2				-Se	-Se
	RC55 CW R.T.		-0.6	-1.0	-1.2				-Se	-Se
	RC55 CW 600° F		-0.6	-1.0	-1.2				-Se	-Se
	RC55 A R.T.	-0.6						-1.2	-1.0	-Se
	RC55 A 600° F			-0.6	-1.0			-1.2	-1.0	-Se
OTHER FERROUS METALS	SANDVIK STEEL (Q-T)			-0.6	-1.0	-1.2			-Se	-Se
	SANDVIK STEEL (N)			-0.6	-1.0	-1.2			-1.2	-1.0
	SAE 1020 STEEL			-0.6	-1.0	-1.2			-1.2	-1.0
	GRAY IRON			-0.6	-1.0	-1.2			-Se	-Se
OTHER NON-FERROUS METALS	24S-T4 AL		-0.6	-1.0	-1.2				-Se	-Se
	J-1 MAGNESIUM	-0.6	-1.0	-1.2					-Se	-Se
NON METAL	GLASS LAMINATE			-0.6	-1.0	-1.2			-Se	-Se

FIG. 14 EXCITING STRESS REQUIRED TO PRODUCE AN EXCITED STRESS NEAR THE FATIGUE STRENGTH FOR SEVERAL STRUCTURAL MATERIALS UNDER UNIFORM STRESS.



$$K_v = \frac{\int \left(\frac{S}{S_e}\right)^2 \frac{dV}{dS} dS}{\int \left(\frac{D}{D_e}\right) \frac{dD}{dS} dS}$$

$$= \frac{\text{Area } \beta}{\text{Area } \alpha}$$

FIG. 15. GRAPHICAL METHOD FOR DETERMINING THE VOLUME-STRESS FACTOR  $K_v$  FOR A PART HAVING COMPLICATED STRESS DISTRIBUTION.

FIG. 16. VOLUME-STRESS FUNCTIONS FOR VARIOUS TYPES OF MEMBERS.

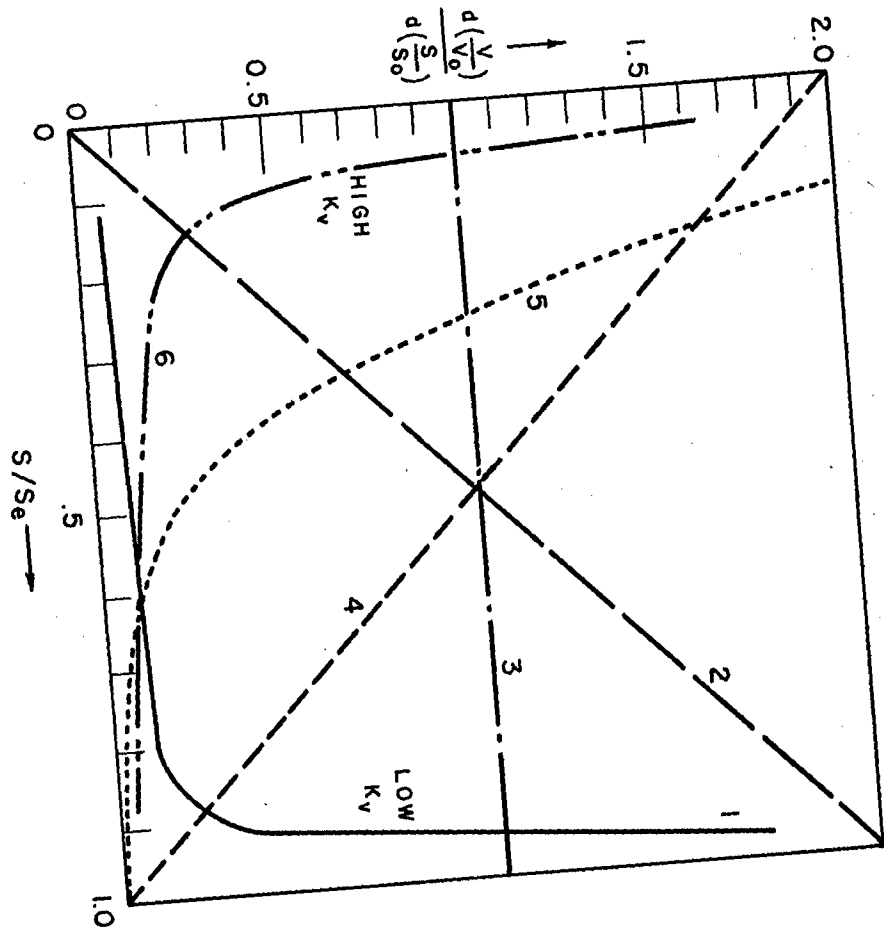
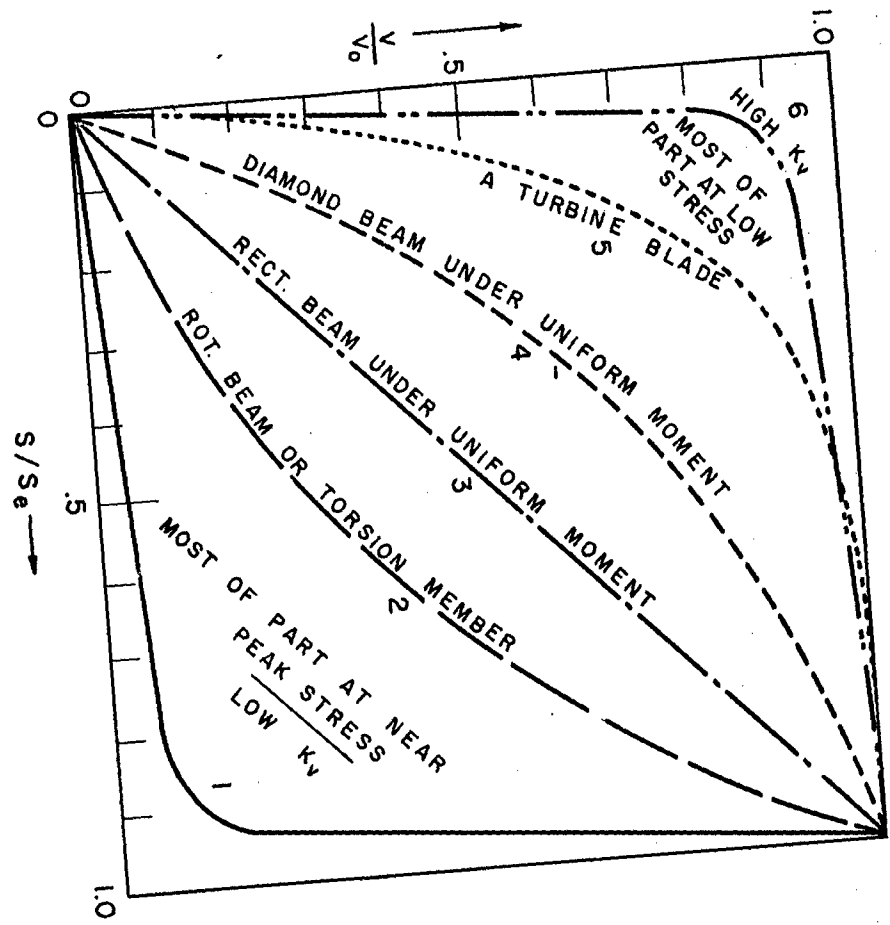
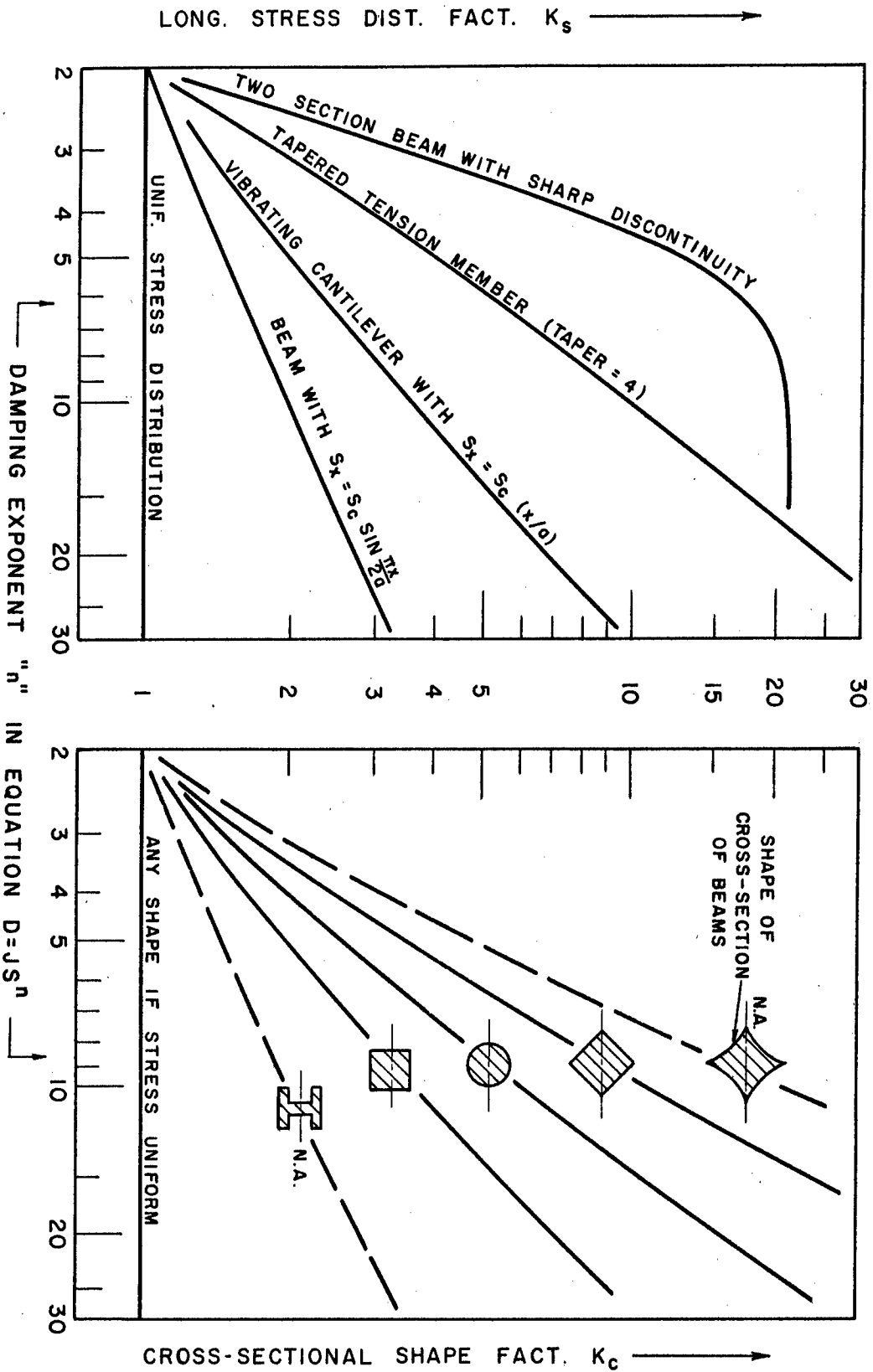


FIG. 17. EFFECT OF DAMPING EXPONENT  $n$  ON LONGITUDINAL STRESS DISTRIBUTION FACTOR AND CROSS-SECTIONAL SHAPE FACTOR OF SELECTED EXAMPLES.



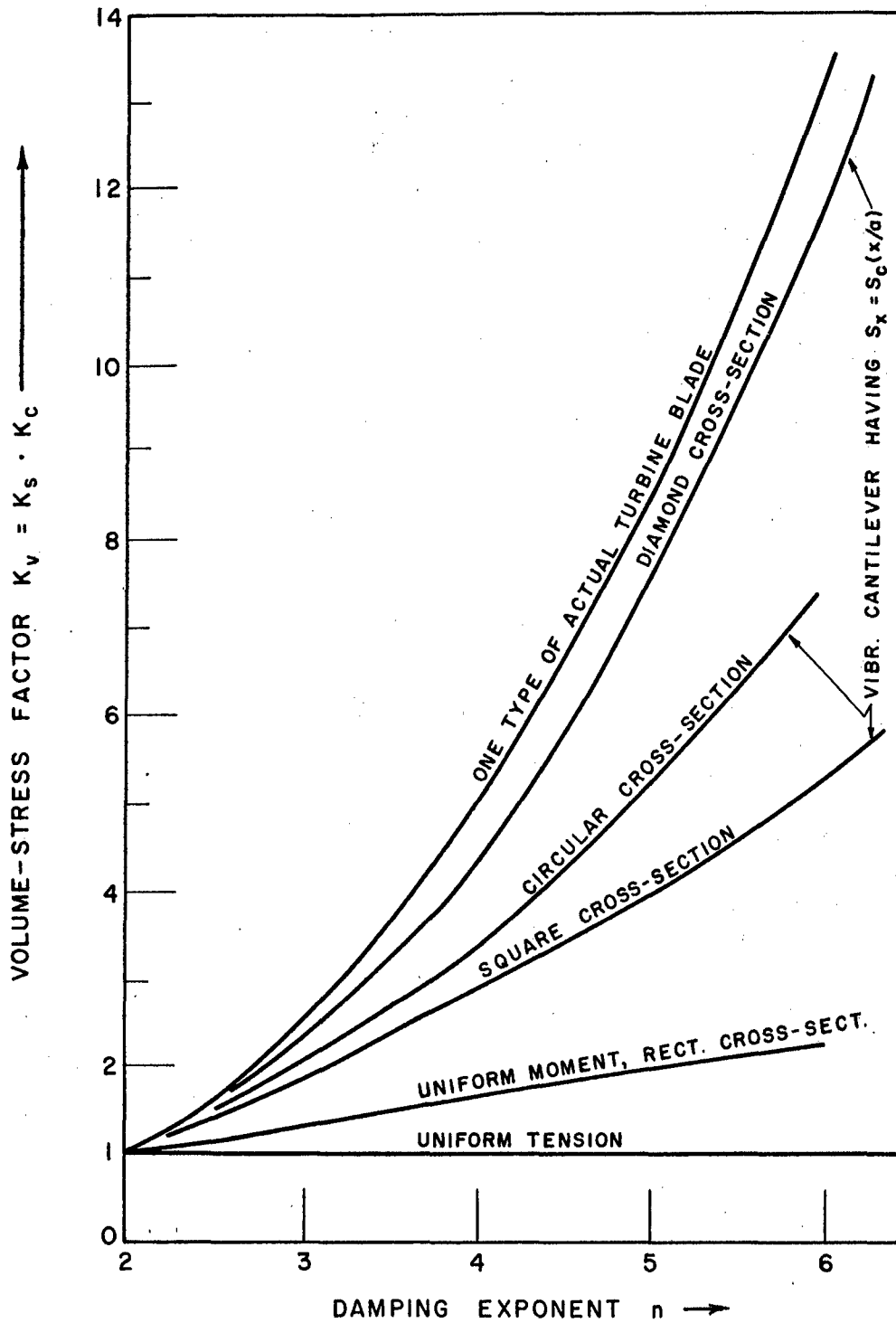


FIG. 18. EFFECT OF DAMPING EXPONENT  $n$  ON VOLUME-STRESS FACTOR OF VARIOUS TYPES OF PARTS.